CCI

BIOMASS

PRODUCT VALIDATION & INTERCOMPARISON REPORT

YEAR 3

VERSION 3.0

DOCUMENT REF:	CCI_BIOMASS_PVIR_V3
DELIVERABLE REF:	D4.1_PVIR
VERSION:	3.0
CREATION DATE:	2021-06-22
LAST MODIFIED	2021-07-29

Document Authorship

	NAME	FUNCTION	ORGANISATION	SIGNATURE	DATE
PREPARED					
PREPARED	A. Araza	WP7	Wageningen University		
PREPARED	S. de Bruin	WP7	Wageningen University		
PREPARED	M. Herold	WP7 Lead	Wageningen University		
PREPARED					
PREPARED					
PREPARED					
PREPARED					
VERIFIED	H. Kay	Project Coordinator	Aberystwyth University		
VERIFIED	R. Lucas	Project Manager	Aberystwyth University		
VERIFIED	S. Quegan	Science Leader	Sheffield University		
APPROVED					

Document Distribution

ORGANISATION	NAME	QUANTITY
ESA	Frank Seifert	

Document History

VERSION	DATE	DESCRIPTION	APPROVED
0.1	2020-12-17	First draft version	
3.0	2021-07-29		

Document Change Record (from Year 1 to Year 2)

VERSION	DATE	DESCRIPTION	APPROVED

TABLE OF CONTENTS

LIST OF TABLES

LIST OF FIGURES

SYMBOLS AND ACRONYMS

AGB	Aboveground biomass
AGB_{map}	Aboveground biomass according to the map
AGB_{ref}	Aboveground biomass from plot, corrected for plot inventory date and if plot size < 1 ha, corrected for partial forest fraction at pixel level
CCI	Climate Change Initiative
CoFor	Congo basin Forests AGB dataset (Ploton et al., 2020)
GNSS	Global Navigation Satellite System
IPCC	Intergovernmental Panel on Clmate Change
I_{Var}	Indicator variable: 1 if the SE_{CCI} is consistent with (Plt), MD and MSD, and 0 otherwise. The latter indicates that the SE_{CCI} layer is overly pessimistic regarding AGB map precision.
LiDAR	LIght Detection And Ranging
MD	Mean difference between AGB_{map} and AGB_{ref}
MSD	Mean square difference (between AGB_{map} and AGB_{ref})
NEON	National Ecological Observatory Network, USA
NFI	National Forest Inventory
PUG	Product User Guide (Santoro, 2020)
PVIR	Product Validation and Inter-comparison Report
PVP	CCI Biomass Product Validation Plan
RMSD	Root mean square difference (between AGB_{map} and AGB_{ref})
SE_{CCI}	Error layer (standard deviation) provided with the CCI Biomass product; if squared denoted as SE_{CCI}^2.
SLB	Sustainable Landscape Brazil
SRTM	Shuttle Radar Topography Mission
TERN	Terrestrial Ecosystem Research Network, Australia
Var(Plt)	Estimated variance of the plot measurement error
Var(S(x))	Estimated variance of the within-pixel sampling error (owing to smaller plot footprint)

1. Introduction

Validation is critical for increasing acceptance of satellite-derived products by the user community. To assess the accuracy of the aboveground biomass (AGB; Mg/ha) estimates of the epochs 2010, 2017 and 2018 of the refined CCI Biomass global products (Santoro, 2021), AGB predictions from the map have been compared with independent AGB data from plots and LiDAR campaigns, which were used as reference values. The main aim of this report is to provide an independent assessment of the quality of the three CCI Biomass products, with this primarily providing (climate) users with uncertainty information when using the map for global and regional climate modelling and assessment purposes. A second purpose is to provide feedback to map producers to establish where the map can be improved.

The reference AGB data are not error-free. *In situ* estimates of AGB are computed based on stem diameter (typically cm), tree height (m), wood density (g cm^3) and allometric models, while geolocation is determined using Global Navigation Satellite System (GNSS) measurements having variable and often limited accuracy. GNSS accuracy is degraded if the paths between the satellites and the GNSS receiver are partly blocked by vegetation cover, which is not uncommon in forests. An additional cause of discrepancies between plots and pixel-based AGB estimates is the difference in support (shape and size) between map pixels and plots. The latter are often much smaller than the pixels they are being compared with, which may introduce two types of error. The first is a *sampling error*, since an estimate of the AGB in only part of the pixel (the plot) is being compared with that of the full pixel. Secondly, and more subtly, a *representation error* can occur if plots are selected with particular properties, such as only being from mature forest despite being in a mixed age forest, so they are not representative of the forest population. This type of representation error is often termed *selection bias*. Both types of error can occur even if the pixel's footprint is fully covered by forest, due to AGB heterogeneity inside the pixel. There may also be a representation error if, for example, a forest plot is used to represent a pixel that is only partially forested. Additionally, the plot inventory date often differs from the biomass map epoch, which gives a temporal mismatch between the compared AGB values.

LiDAR-based AGB estimates used as reference data can completely cover map pixels or even larger pixel blocks, which minimizes the sampling errors referred to above. However, just like the *in situ* estimates of AGB, LiDAR-based AGB values are themselves predictions, so are subject to prediction error that has to be taken into account.

Each of the above-mentioned factors can introduce errors with a random or a systematic nature. The latter type of error is of particular concern since it cannot be reduced by aggregating individual tree measurements over large plots or by averaging small plot data over many plots. Systematic errors in reference data have to be reduced as much as possible by adhering to a standardized measurement protocol (CEOS, 2021).

The three versions of the CCI Biomass Product Validation Plan (PVP; de Bruin et al., 2019a, 2020, 2021) presented approaches for addressing the temporal mismatch between plot and pixel data and partial forest fractions within map pixels. The reports also proposed methods for assessing the variance of the other error sources. In this third PVIR, the temporal mismatch between plot and pixel data and partial forest fractions within map pixel are handled similarly to the first two PVIRs. The proposed approaches for accounting for other error sources are partly implemented, up to the point supported by available data.

An extensive dataset of forest plot data across the world was acquired for the purpose of the validation (see Appendix A, Figure 1 and Table 1). As before, the plots underwent a series of quality checks (see Section 2.1). Forest plot data and LiDAR were not used to calibrate the CCI Biomass map in order to guarantee full independence from the production process. The contributions of AGB measurement error and spatial representation error are known to be largest for small plots, such as those typical of National Forest Inventories (NFIs), while detailed measurements of all trees within large plots are expected to deliver the highest quality AGB data (Réjou-Méchain et al., 2019; Réjou-Méchain et al., 2014). To take into account expected differences in the accuracy of plot data, a Tiered approach was chosen which comprised:

- Tier 1 - small plots (≤ 0.6 ha), including NFI data,
- Tier 2 - larger plots (0.9-3 ha; Tier 2), and

- Tier 3- high-quality large super-plots (≥ 6 ha; mainly from Labrière et al. (2018)).

The Tiers were analysed separately in the plot-pixel comparisons. AGB map comparisons with data derived from LiDAR and aggregated plot data (see Section 2.2) were also analysed separately.

The map inter-comparison presented in this document concerns consistency of map-reference deviations amongst the three current CCI Biomass AGB products and comparisons with Version 2 of the CCI Biomass products (Santoro, 2020). Results from two external map inter-comparison as examples of user-led independent validation are also included.

2. Materials and methods

2.1. Forest plot data

For CCI Biomass, new forest inventory and plot data from research networks were added to the previously established GlobBiomass reference database (Rozendaal et al., 2017). Reference data were only included if quality criteria, as described in the PVP, were met. Specifically, the plots needed:

- A citable reference source and metadata to assess the procedures and quality of biomass estimation.
- Precise coordinates (4-6 decimals for coordinates in decimal degrees of plot centroids).
- A census date within ten years of the reference year of the AGB map to avoid temporal inconsistency with the assessed maps.
- Inclusion of measurements of all trees of diameter ≥ 10 cm (or less).
- To have experienced no deforestation between the year of the inventory and the reference year of the CCI Biomass map (i.e., 2010, 2017 and 2018). This was assessed based on the 2018 forest loss layer of the Hansen dataset (Hansen et al., 2013).

Table 1 lists the numbers of plots used in each Tier and for each of the map reference years.

Table 1. Number of plots used in each Tier for the different AGB map reference years.

Map ref. year	Tier1	Tier2	Tier3	Total
2010	119744	716	27	120487
2017	70598	536	23	71157
2018	70540	464	21	71025

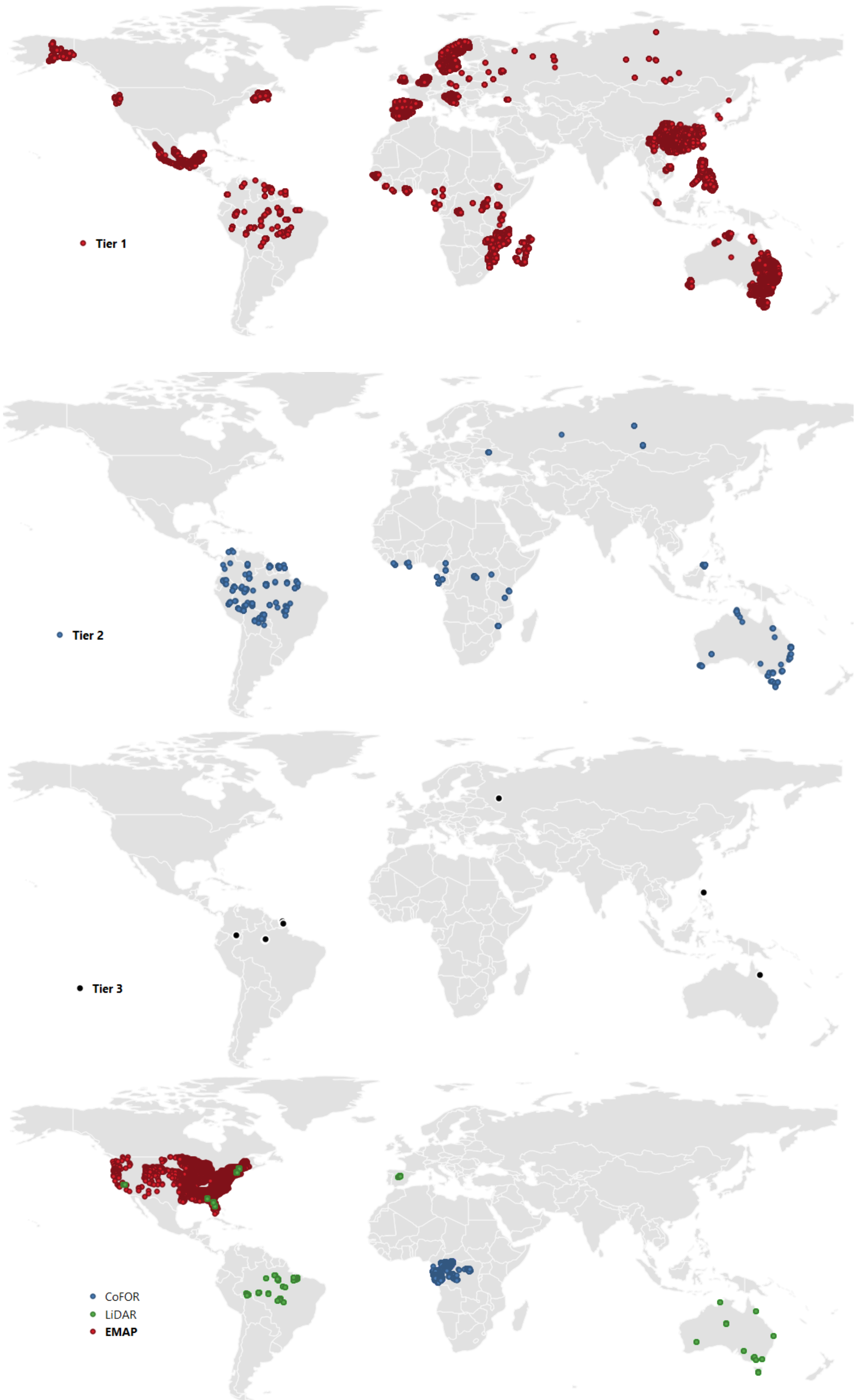

Figure 1. Geographical locations of plots and footprints of the reference datasets (CoFor = Congo basin Forests, LiDAR and EMAP = Environmental Monitoring and Assessment Program).

2.2. AGB estimates from LiDAR, Congo basin management inventories, and US Forest Service plots

In addition to the plot data, we used LiDAR-based AGB data at 100 m resolution from the Sustainable Landscape Brazil project (SLB), the National Ecological Observatory Network, USA (NEON) and the Terrestrial Ecosystem Research Network, Australia (TERN), which were processed by Labrière and Chave (2020a, b, c). The 1-km pixel forest management inventory data used in this report originated from the Congo basin Forests AGB (CoFor) dataset (Ploton et al., 2020). For the CoFor dataset, only pixels having at least five *in situ* forest management inventoried plots were used. Lastly, we used the Environmental Monitoring and Assessment Program (EMAP) AGB aggregates of 27-km hexagons estimated from the Forest Inventory and Analysis Program of the US Forest Service (Menlove and Healey, 2020), which was useful only for 2017 and 2018 analysis.

Table 2 lists the numbers of LiDAR, CoFor and EMAP footprints used in each Tier and for each of the map reference years.

Table 2. Number of LiDAR, CoFor and EMAP footprints used for the different AGB map reference years.

Map ref. year	CoFor	LiDAR	EMAP	Total
2010	16896	155444	-	172340
2017	9356	1037218	3874	1050448
2018	8777	1040529	2118	1051424

As described in the PVPs, we rely on opportunistic AGB plot data that were not specifically produced for validation purposes but that are rather collected within the context of country NFIs and research efforts at local to regional scales.

2.3. Preparation of validation datasets

Temporal harmonization

Differences between the inventory date of AGB plots and the reference year of the AGB map were harmonized using updated IPCC growth rates (IPCC, 2019; Requena Suarez et al., 2019) following the approach described in Version 1 of the PVP. For plots in tropical and subtropical ecological zones, age-category-dependent growth rates are available (IPCC, 2019; Requena Suarez et al., 2019). In those cases, plot AGB values in the range 0-99 Mg/ha were assumed to represent young secondary forest, AGB values in the range 100-128 Mg/ha were treated as old secondary forest (Van Breugel et al., 2007), and AGB above 129 Mg/ha was assumed to correspond to old growth stands (Brown et al., 1989; Clark & Clark, 2000; Mello et al., 2016). Given the absence of data on plot forest age, low biomass but mature forests could not be distinguished from young stands, with potential implications for the applied growth rates. For temperate oceanic forests in Europe and boreal coniferous forests and tundra woodlands, no differentiation of growth rates over age categories was used. The temporal adjustments by growth rates were applied up to a difference of ten years between the inventory date and the map reference year. Plots having a longer temporal difference were discarded in the analyses. The LiDAR dataset was exempted from temporal adjustment because it contained repeated measurements between 2011 and 2018.

Correction for forest fraction

As described in the PVP, correction for inclusion of non-forested areas within map pixels was undertaken by multiplying the temporally adjusted plot AGB by forest fraction at the pixel level. This forest fraction was computed by setting a 10% threshold on the 2010 tree cover product (Hansen et al., 2013), which had a resolution of 1 arc-second per pixel, or approximately 30 meters per pixel at the equator. In the rare case of more than one AGB plot within a pixel, the average of the adjusted AGB per plot was used. The correction for forest fraction was only applied to plots with an area below 1 ha.

Comparisons at 0.1° cell resolution

To reduce the effect of short-range AGB variations in the map and their potential interaction with plot-map geolocation mismatches and to assess the CCI Biomass map at a resolution commonly used by climate modellers, AGB_{map} - AGB_{ref} comparisons from Tier 1 data were also made over multi-pixel blocks at 0.1° cell resolution. In this case, correction for partial forest fraction (see above) was undertaken at the level of the coarse resolution cells. Mean AGB_{ref} at 0.1° cell level was computed by multiplying forest fraction at the 0.1° cell level by the mean temporally adjusted AGB of at least five plots in that cell. The procedure is illustrated in Figure 5 of the PVP (de Bruin et al., 2019a). The AGB reference values thus obtained were compared with the average map AGB spatially aggregated over the 0.1° cells. In the case of the EMAP dataset comparison, we averaged the map AGB to 0.25°.

The correction for forest fraction was not applied to the LiDAR dataset since the LiDAR footprints were assumed to representatively sample forest/non-forest fractions within the 0.1° cells, i.e., forested areas were not preferentially sampled.

Ecoregions / biomes

AGB_{map} - AGB_{ref} comparisons at 0.1° cell resolution were also stratified according to ecoregions derived from a recent global ecoregion map (Dinerstein et al., 2017), which wasdownloaded from https://ecoregions2017.appspot.com/. The original vector maps were rasterized to 0.1° resolution. Resulting raster cells were assigned to the category covering the largest portion of the cell area. We stratified comparisons from Tier 3 data at 0.1° cell resolution per biome.

2.4. Comparing AGB map pixels with reference data

Assumptions

After adjustments for temporal discrepancies and partial forest fraction and having at least ten plots within a reference biomass range, we assumed unweighted means computed from reference data in Tiers 1 and 2 to be unbiased. The biomass ranges used are listed in the first column of Table 2. For Tier 3 data, we relaxed the requirement of ten plots per biomass range because these data were recorded over large plots (≥ 6 ha) and followed a strict measurement protocol. Under the unbiasedness assumption, mean differences between harmonized plot data and map values aggregated over bins covering ranges of reference AGB values are interpreted as *map bias*. To empirically verify the assumption of unbiased plot data, we conducted the analyses for each of the three Tiers and assessed consistency of results over the three Tiers, whenever data volume allowed us to do so.

When reporting mean differences (MD) and (root) mean square difference ((R)MSD) over ecoregions, we assume that plot-map comparisons within ecoregions are representative of those regions.

To facilitate a preliminary assessment of the standard deviation layer accompanying the CCI Biomass maps (see below), we assumed map error and plot measurement error to be spatially uncorrelated and mutually uncorrelated. This assumption was made because, at the time of writing this report, we had only limited data for assessing spatial correlation structures of the error components (see sections 2.5 and 2.6).

Measures

Besides reporting mean differences between reference and map AGB per biomass range, which are interpreted as map bias (see above), we also report (root) mean square deviations (MSD) between map values and plots. At this stage, we did not interpret MSD as the mean square *error* of the map since we will elaborate on the assessment of the variance of individual error components in later stages of the project. However, we did assess whether the mean variance of map error ($mean(SE^2_{CCI})$)—where SE_{CCI} is the standard error layer provided with the CCI Biomass AGB map—is consistent with

MSD, *MD* and the mean variance of plot measurement error $mean(Var(Plt))$. The SE_{CCI} layer only represents the random part of AGB errors (Santoro, personal communication). Leaving out three random error components listed in the PVP (positional error, within-pixel representation error and the data harmonization error) and under the assumptions given above, we checked whether

$$mean(SE_{CCI}^2) \leq MSD - MD^2 - mean(Var(Plt)).$$

For this purpose, we defined an indicator variable I_{Var}, as follows:

$$I_{Var} = \begin{cases} 1 \;\; if \; mean(SE_{CCI}^2) \leq MSD - MD^2 - mean(Var(Plt)) \\ \qquad\qquad\qquad 0 \quad otherwise \end{cases}$$

If I_{Var} has value zero, $mean(SE_{CCI}^2)$ would be too large or, in other words, the SE_{CCI} layer provided with the biomass product would be pessimistic about map precision, unless the variance of plot measurement error is greatly underestimated.

For plots having tree-level data, (Plt) was computed using the Réjou-Méchain et al. (2017) biomass R-package. For other plots lacking such data, $Var(Plt)$ was predicted by a random forest model trained on the plots having tree-level data, using plot biomass, plot size, general and specific eco-zones and continent as explanatory variables.

2.5. Spatial correlation of AGB

Experimental semi-variograms were computed and variogram models were fitted using gstat (Pebesma, 2004) based on LiDAR-AGB data acquired over two forest sites in Remningstorp, Sweden, and Lope, Gabon, i.e., a *boreal* and a *tropical* forest site. These ALS datasets were acquired in the framework of the airborne ESA BIOSAR (Ulander et al., 2011) and AfriSAR (Hajnsek et al., 2017) campaigns to provide detailed information on forest vertical structure and to produce high-resolution AGB maps. The AGB data have a spatial resolution of 10 m (Remningstorp) and 20 m (Lope) and were also used in version 2 of the Product User Guide (PUG; Santoro, 2020). Non-forest areas (such as savanna in the Lope study area) were masked out after manually digitizing forested areas using high resolution Google Earth imagery. Accordingly, the variogram models represent spatial correlation of AGB within forested areas at the study sites.

2.6. Effect of spatial support on sampling error and suggested map bias

The variogram models described above were used to assess the effects of the within-pixel sampling error (see Introduction) for the forest sites in Remningstorp and Lope. This was undertaken by two means:

- By computing the variance of the difference between sub-pixel plots and plot configurations (i.e., for plots smaller than pixels) and AGB map pixels at locations x as:

$$\begin{aligned} Var(S(x)) &= Var\left(AGB_{ref}(x) - AGB_{map}(x)\right) \\ &= Var(AGB_{ref}) + Var(AGB_{map}) - 2 * Cov(AGB_{ref}, AGB_{map}), \end{aligned}$$

  where $Var(AGB_{ref})$ is the sill of the variogram at the spatial support of the plots, $Var(AGB_{map})$ is the within-pixel covariance, and $Cov(AGB_{ref},\ AGB_{map})$ is the plot to pixel covariance. Note that for brevity reference to the location x is omitted in the right-hand side of the above equation. Plot to pixel covariance are computed using the geostatistical framework for change of support (Kyriakidis, 2010).

- By simulating possible plot AGB, conditional on given AGB values at the pixel level, using the $Var(AGB_{ref} - AGB_{map})$ computed in the above step. The aim of this simulation is to reproduce and explain results in Section 3.3 of the PUG (Santoro, 2020) by a geostatistical approach.

3. Validation results for the global maps

3.1. Global assessments per Tier of plot data

Tier 1 non-aggregated

The non-aggregated results (i.e., at original resolution) of global plot-map comparisons using Tier 1 data (plot size ≤ 0.6 ha) are shown in Figure 2 and Tables 3-5.

An overall feature of the comparisons is over-prediction of low reference biomass and under-prediction of higher reference biomass values, while relative accuracy is within 20% in the middle range. On average, under-prediction by the map starts occurring at a reference biomass of approximately 160 Mg/ha but the interquartile range of plot data still covers the 1:1 line between AGB_{ref} and AGB_{map} up to approximately 275 Mg/ha. The under-prediction increases with reference biomass and reaches maxima of 476 Mg/ha (2010), 421 Mg/ha (2017) and 421 (2018) for mean reference biomass densities of 610, 612 and 613 Mg/ha, respectively. The latter values originate from small plots with exceptionally high biomass that are unlikely to cover extensive areas and are unlikely to be captured by the biomass retrieval algorithm. The banding observed in the left column of Figure 2 seems to be caused by a maximum AGB level set for particular regions in the retrieval algorithm. A first impression is that the accuracy of the current map versions has improved with respect to the previous edition reported in de Bruin et al. (2020b: Table 4 and Figure 4 therein). This is further analysed in Section 3.8.

As noted in the PUG (Santoro, 2020), the within-pixel sampling error contributes to the observed over-prediction of low reference AGB and under-prediction of higher reference AGB values, even if the mean AGB of the population from which the small plot is drawn agrees with the map at pixel level. This is elaborated on in Section 3.9.

In all cases but the two bottom rows of Tables 3-4, the indicator variable $I_{Var} = 0$, suggesting the SE_{CCI} layer provided with the AGB product is pessimistic about the precision of the CCI Biomass 2017 map. The considerable mean variance of plot measurement error, $mean(Var(Plt))$, of the smallest plot size category definitely contributes to this observation. Only for the highest reference AGB value does I_{Var} attain the value 1. Further analyses of the random error components are needed to assess whether the reported SE_{CCI} for $AGB_{ref} > 400$ Mg/ha is indeed reasonable.

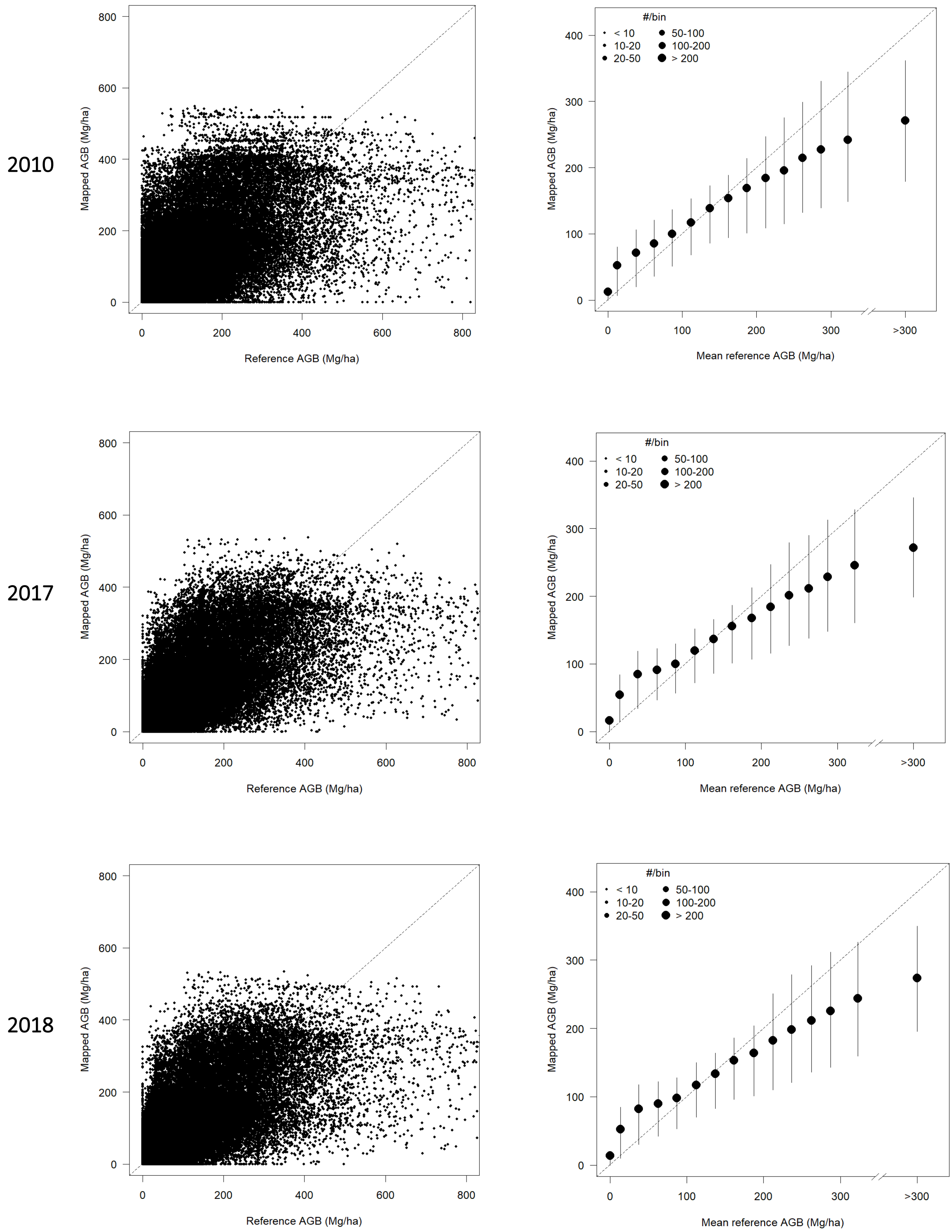

Figure 2. Plot-map comparisons for Tier 1 data at original resolution (i.e., without spatial aggregation) for the three AGB maps; left column: scatterplots; right column: binned over 25 Mg/ha wide biomass ranges with whiskers representing the interquartile range of mapped biomass values. AGB_{ref} > 350 Mg/ha data are grouped into a single bin. Note the different scales on the left and right

graphs.

Table 3. Validation results per biomass range for Tier 1 data at original resolution for the 2010 map.

AGB_{ref} bin	# plots	AGB_{ref}	AGB_{map}	*MD*	*RMSD*	*MSD*	$Var(Plt)^a$	$SE^2_{CCI}{}^a$	I_{Var}
[Mg/ha]	count	---------------------[Mg/ha]			---------------------	--------------[Mg/ha]^2		------------------	-
0-50	53604	15	43	27	58	3389	8735	5568	0
50-100	29688	73	92	19	66	4366	10419	12508	0
100-150	16390	122	126	4	78	6094	12964	23212	0
150-200	7487	173	161	-12	96	9307	17438	38007	0
200-250	4489	223	189	-34	114	13011	16101	51188	0
250-300	2867	273	220	-53	127	16140	16520	63784	0
300-400	2892	342	248	-94	153	23398	18769	75926	0
>400	2327	762	278	-484	832	692462	47663	91726	1
total	119744	90	93	2	138	18911	11737	18210	1

[a] simplified notation; referring to means over biomass ranges

Table 4. Validation results per biomass range for Tier 1 data at original resolution for the 2017 map.

AGB_{ref} bin	# plots	AGB_{ref}	AGB_{map}	*MD*	*RMSD*	*MSD*	$Var(Plt)^a$	$SE^2_{CCI}{}^a$	I_{Var}
[Mg/ha]	count	---------------------[Mg/ha]			---------------------	--------------[Mg/ha]^2		------------------	-
0-50	22158	18	53	35	61	3745	15645	2481	0
50-100	17097	75	96	21	64	4084	17351	4939	0
100-150	13100	125	128	3	74	5446	18020	9468	0
150-200	6133	173	161	-12	86	7312	21425	15135	0
200-250	3785	223	192	-31	102	10441	19207	21606	0
250-300	2515	274	220	-54	115	13308	18848	26378	0
300-400	2698	342	250	-92	139	19300	19461	33370	0
>400	2158	770	278	-491	848	718590	48323	34538	1
total	69644	122	115	-7	167	27924	18489	9605	1

[a] simplified notation; referring to means over biomass ranges

Table 5. Validation results per biomass range for Tier 1 data at original resolution for the 2018 map.

AGB_{ref} bin [Mg/ha]	# plots count	AGB_{ref}	AGB_{map}	MD	$RMSD$	MSD	$Var(Plt)$[a]	SE^2_{CCI}[a]	I_{Var}
		[Mg/ha]				[Mg/ha]^2			-
0-50	22049	18	51	32	60	3652	15666	2923	0
50-100	17167	75	94	19	65	4220	17285	6104	0
100-150	13091	125	125	1	74	5502	18001	10896	0
150-200	6141	173	158	-15	88	7741	21388	17629	0
200-250	3780	223	189	-34	105	11022	19215	24510	0
250-300	2514	274	218	-56	119	14055	18817	30149	0
300-400	2691	342	250	-93	141	19932	19501	38475	0
>400	2153	770	281	-489	846	715547	48433	39137	1
total	69586	122	113	-9	167	27933	18478	11157	1

[a] simplified notation; referring to means over biomass ranges

Table 6. Validation results per biomass range for Tier 2 data at original resolution for the 2010 map.

AGB_{ref} bin [Mg/ha]	# plots count	AGB_{ref}	AGB_{map}	MD	$RMSD$	MSD	$Var(Plt)$[a]	SE^2_{CCI}[a]	I_{Var}
		[Mg/ha]				[Mg/ha]^2			-
0-50	61	21	71	50	113	12864	1938	29247	0
50-100	55	73	153	79	137	18797	211	32359	0
100-150	75	127	202	75	119	14203	370	45142	0
150-200	73	174	253	79	132	17408	1354	49542	0
200-250	104	228	286	58	128	16373	2062	65564	0
250-300	96	274	334	60	137	18853	713	95407	0
300-400	128	346	315	-31	134	18034	750	88263	0
>400	124	592	309	-283	381	145258	7530	80085	1
total	716	273	261	-12	198	39089	2191	66721	0

[a] simplified notation; referring to means over biomass ranges

Tier 2 non-aggregated

The non-aggregated results (i.e., at original resolution) of global plot-map comparisons using Tier 2 data (plot sizes 0.9 – 3 ha) are shown in Figure 3 and Tables 6-8. Spatial aggregation to 0.1° cells was omitted for this Tier because of the limited number of available Tier 2 plots.

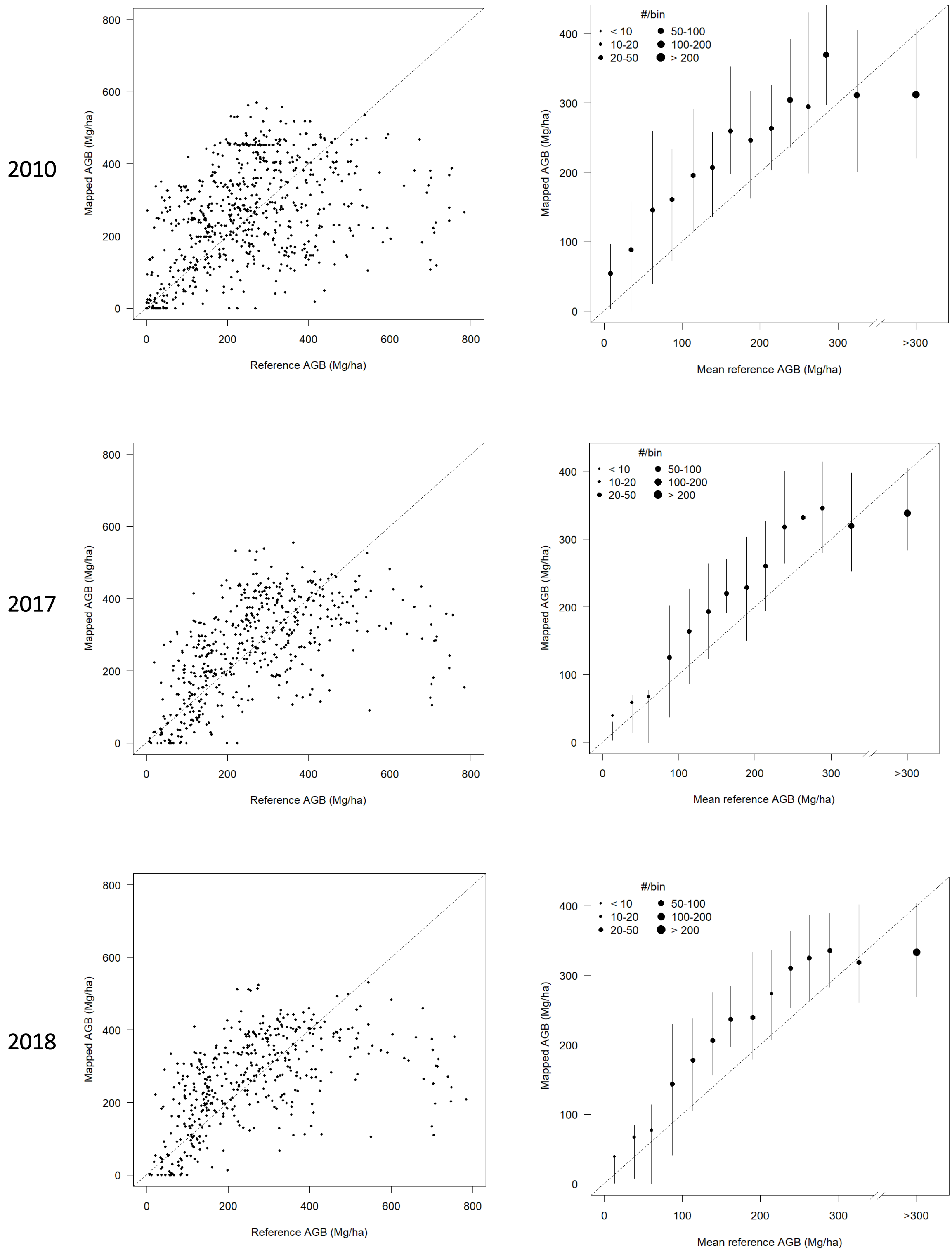

Figure 3. Plot-map comparisons for Tier 2 data at original resolution (i.e., without spatial aggregation); left column: scatterplots; rights column: binned over 25 Mg/ha wide biomass ranges with whiskers representing the interquartile range of mapped biomass values and symbol size representing the number of plots per biomass range. AGB_{ref} > 350 Mg/ha data are grouped into a single bin. Note the different scales on the left and right graphs.

Table 7. Validation results per biomass range for Tier 2 data at original resolution for the 2017 map.

AGB$_{ref}$ bin	# plots	AGB$_{ref}$	AGB$_{map}$	MD	$RMSD$	MSD	$Var(Plt)$[a]	SE^2_{CCI}[a]	I_{Var}
[Mg/ha]	count	---------------------[Mg/ha]	---------------------			-------------[Mg/ha]^2	-----------------		-
0-50	23	30	52	22	73	5396	770	4971	0
50-100	46	78	104	26	97	9363	305	8447	1
100-150	77	127	180	53	103	10620	323	13989	0
150-200	54	174	224	50	106	11298	489	17085	0
200-250	54	230	297	67	123	15140	1649	32066	0
250-300	70	274	338	64	113	12850	624	39905	0
300-400	99	345	324	-21	99	9764	658	43488	0
>400	113	597	341	-256	374	139723	7783	42503	1
total	536	292	265	-27	195	38162	2165	30104	1

[a] simplified notation; referring to means over biomass ranges

Table 8. Validation results per biomass range for Tier 2 data at original resolution for the 2018 map.

AGB$_{ref}$ bin	# plots	AGB$_{ref}$	AGB$_{map}$	MD	$RMSD$	MSD	$Var(Plt)$[a]	SE^2_{CCI}[a]	I_{Var}
[Mg/ha]	count	---------------------[Mg/ha]	---------------------			-------------[Mg/ha]^2	-----------------		-
0-50	23	30	58	28	82	6716	770	6990	0
50-100	47	78	119	42	110	12188	546	12458	0
100-150	77	127	194	66	107	11510	324	15925	0
150-200	47	174	238	64	108	11683	392	18264	0
200-250	45	229	296	67	111	12392	1773	33515	0
250-300	54	274	330	56	103	10684	486	38007	0
300-400	83	345	322	-23	96	9298	568	52662	0
>400	88	638	335	-303	416	173211	9625	45360	1
total	464	285	260	-25	204	41620	2342	31798	1

[a] simplified notation; referring to means over biomass ranges

In general, over-prediction of biomass is observed for reference biomass values up to 300 Mg/ha, unlike the previous edition where over-prediction was observed until 200 Mg/ha. Biomass is under-predicted by this current edition of CCI Biomass maps above 350 Mg/ha. The under-prediction increases with reference biomass and reaches maxima of 326 Mg/ha (2010), 311 Mg/ha (2017) and 292 Mg/ha (2018) for mean reference biomass densities of 543, 538 and 539 Mg/ha, respectively.

In most cases, the indicator variable $I_{Var} = 0$ despite the $mean(Var(Plt))$ estimates of larger plots in Tier 2 being much lower than the previous Tier. This implies that the SE_{CCI} layer provided with the biomass product is still *pessimistic* about the precision of the CCI Biomass maps.

Tier 3 non-aggregated

The non-aggregated results (i.e., at original plot level) of global plot-map comparisons using Tier 3 data (plot size ≥ 6 ha) are shown in Figure 4 and Tables 9-11. Similar to Tier 2, spatial aggregation to 0.1° cells was omitted because of the small number of available Tier 3 plots.

It is important to note that most Tier 3 plots are in the tropics and cover a biomass range between 150 and 450 Mg/ha (i.e., the biomass range where SAR sensors lose sensitivity), and so lack low biomass densities. The small number of plots and the large scatter hardly allow conclusions to be drawn based on these data, except for the general trend of the map to under-predict AGB in the higher part of the assessed AGB range, which was also observed with the Tier 1 & 2 data.

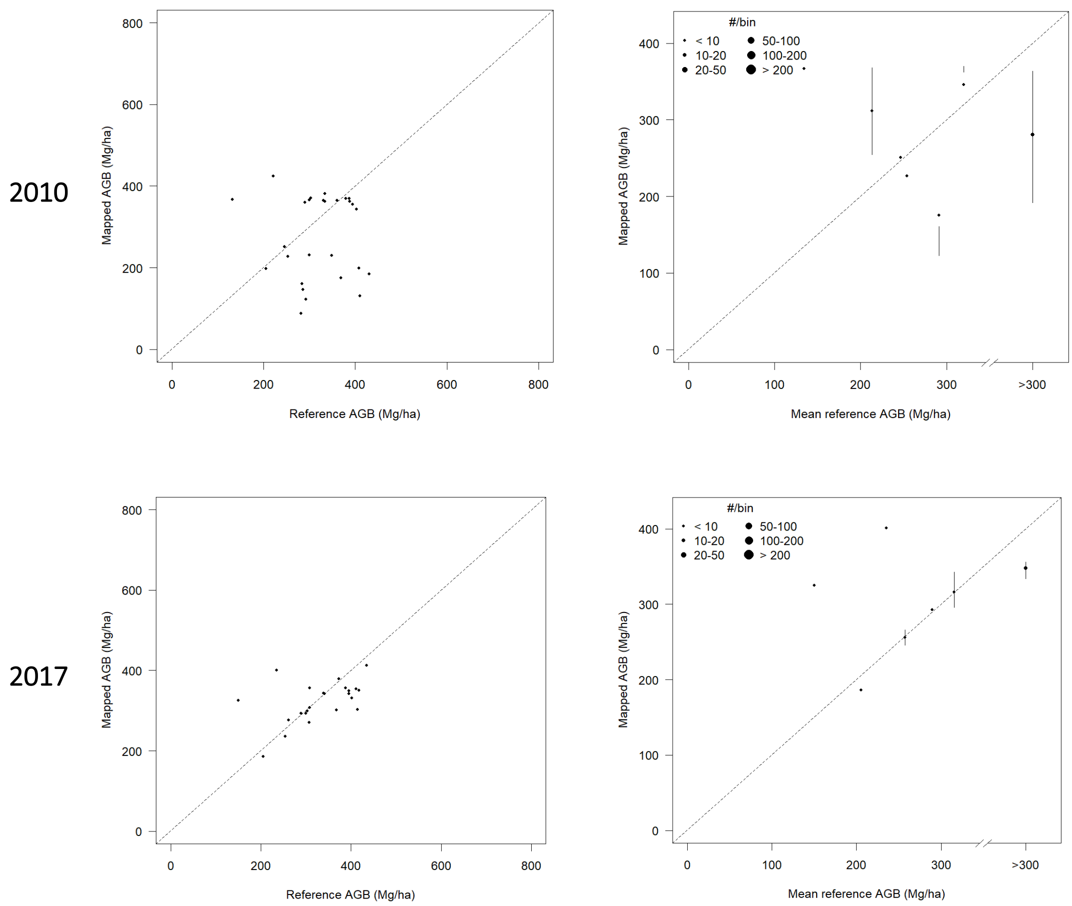

2018

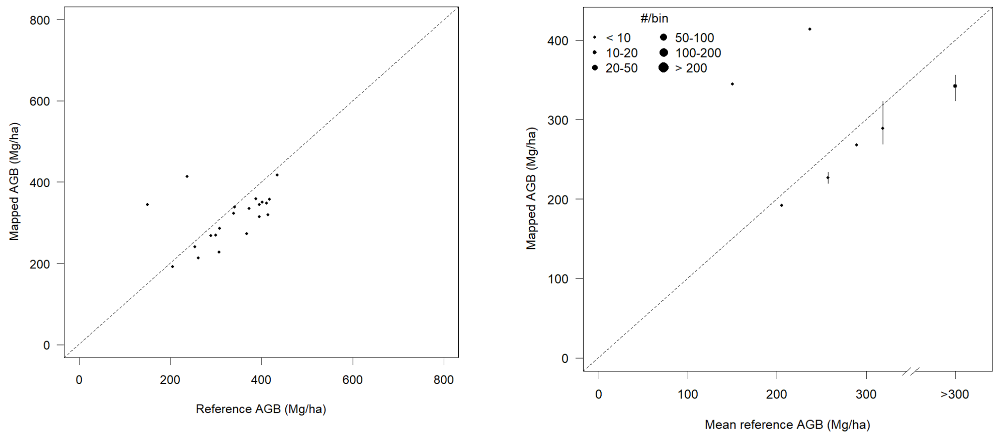

Figure 4. Plot-map comparisons for Tier 3 data at original resolution (i.e., without spatial aggregation); left column: scatterplots; right column: binned over 25 Mg/ha wide biomass ranges with whiskers representing the interquartile range of mapped biomass values and symbol size representing the number of plots per biomass range. AGB_{ref} > 350 Mg/ha data are grouped into a single bin. Note the different scales in the left and right graphs.

Table 9. Validation results per biomass range for Tier 3 data at the original resolution for the 2010 map.

AGB_{ref} bin	# plots	AGB_{ref}	AGB_{map}	MD	$RMSD$	MSD	$Var(Plt)$[a]	SE^2_{CCI}[a]	I_{Var}
[Mg/ha]	count	---------------------[Mg/ha]	---------------------			--------------[Mg/ha]^2	------------------		
0-50	-	-	-	-	-	-	-	-	-
50-100									
	1	134	367	233	233	54216	123	51529	1
150-200	-	-	-	-	-	-	-	-	-
200-250	3	225	291	67	118	13858	666	70109	0
250-300	6	285	184	-101	136	18520	492	14948	1
300-400	13	350	331	-19	74	5500	319	88047	0
>400	4	413	214	-198	215	46133	266	44769	1
total	27	323	278	-45	131	17146	381	62045	0

[a] simplified notation; referring to means over the biomass ranges

Table 10. Validation results per biomass range for Tier 3 data at the original resolution for the 2017 map.

AGB_{ref} bin	# plots	AGB_{ref}	AGB_{map}	MD	$RMSD$	MSD	$Var(Plt)$[a]	SE^2_{CCI}[a]	I_{Var}
[Mg/ha]	count	---[Mg/ha]---				---[Mg/ha]^2---			
0-50	-	-	-	-	-	-	-	-	-
50-100	-	-	-	-	-	-	-	-	-
100-150	-	-	-	-	-	-	-	-	-
150-200	1	150	325	175	175	30535	213	21609	1
200-250	2	220	294	73	118	13922	985	21825	0
250-300	3	268	268	0	14	183	231	11269	0
300-400	12	344	328	-15	34	1182	381	17669	0
>400	5	416	350	-66	72	5149	294	24876	0
total	23	331	322	-8	66	4298	388	18933	0

[a] simplified notation; referring to means over the biomass ranges

Table 11. Validation results per biomass range for Tier 3 data at the original resolution for the 2018 map.

AGB_{ref} bin	# plots	AGB_{ref}	AGB_{map}	MD	$RMSD$	MSD	$Var(Plt)$[a]	SE^2_{CCI}[a]	I_{Var}
[Mg/ha]	count	---[Mg/ha]---				---[Mg/ha]^2---			
0-50	-	-	-	-	-	-	-	-	-
50-100	-	-	-	-	-	-	-	-	-
100-150	-	-	-	-	-	-	-	-	-
150-200	1	150	345	195	195	37925	213	28900	1
200-250	2	221	303	82	125	15706	1008	44810	0
250-300	3	268	241	-27	31	977	231	11390	0
300-400	10	351	307	-44	53	2831	259	23072	0
>400	5	416	359	-57	63	3907	294	34741	0
total	21	333	311	-22	76	5720	332	26529	0

[a] simplified notation; referring to means over the biomass ranges

3.2.Tier 1 plot data spatially aggregated to 0.1° cells

The results of global AGM_{map} - AGB_{ref} comparisons using Tier 1 data (plot size ≤ 0.6 ha) spatially aggregated to 0.1° cells are shown in Figure 5 and Tables 12-14. The rightmost variance columns shown in Tables 3-11 are omitted here because spatial correlation of errors within 0.1° cells may be non-negligible, but we lack data to assess such correlation for most biomes at the current stage of the project.

Spatial aggregation to 0.1° cells improved the fit between AGB_{ref} and AGB_{map} with absolute mean differences within 30 Mg/ha below 300 Mg/ha. Beyond 300 Mg/ha, AGB values are still under-predicted and the 0.1° cells producing the most under-prediction are located in southeast Australia. These cells show lower estimates than the previous version of CCI Biomass (not shown here). The results of the three epochs for version 3 of the CCI maps show more consistency than their previous versions (see Section 3.8 for further analysis of consistency).

Spatial aggregation reduced the effect of localized AGB fluctuations in the map and their potential interaction with plot-map geolocation mismatches. These results (Figure 5, Tables 12-14) suggest the CCI Biomass predictions at 0.1° cell resolution are more accurate than at the original pixel resolution. As we will see later, very similar results were obtained for the temperate broadleaf and mixed forest biome. Most 0.1° cells meeting the criterion of at least five plots per cell happen to be located in that biome.

Table 12. Validation results per biomass range for Tier 1 data spatially aggregated to 0.1° cells for the 2010 map.

AGB_{ref} bin [Mg/ha]	# cells count	AGB_{ref}	AGB_{map}	*MD*	*RMSD*
		---------------------[Mg/ha]	---------------------		
0-50	4090	23	36	13	30
50-100	1695	70	80	11	34
100-150	482	121	138	16	70
150-200	234	172	197	25	84
200-250	139	226	241	14	88
250-300	96	273	273	1	76
300-400	56	336	259	-77	113
>400	51	692	277	-415	497
total	6843	62	71	9	60

2010

2017

2018

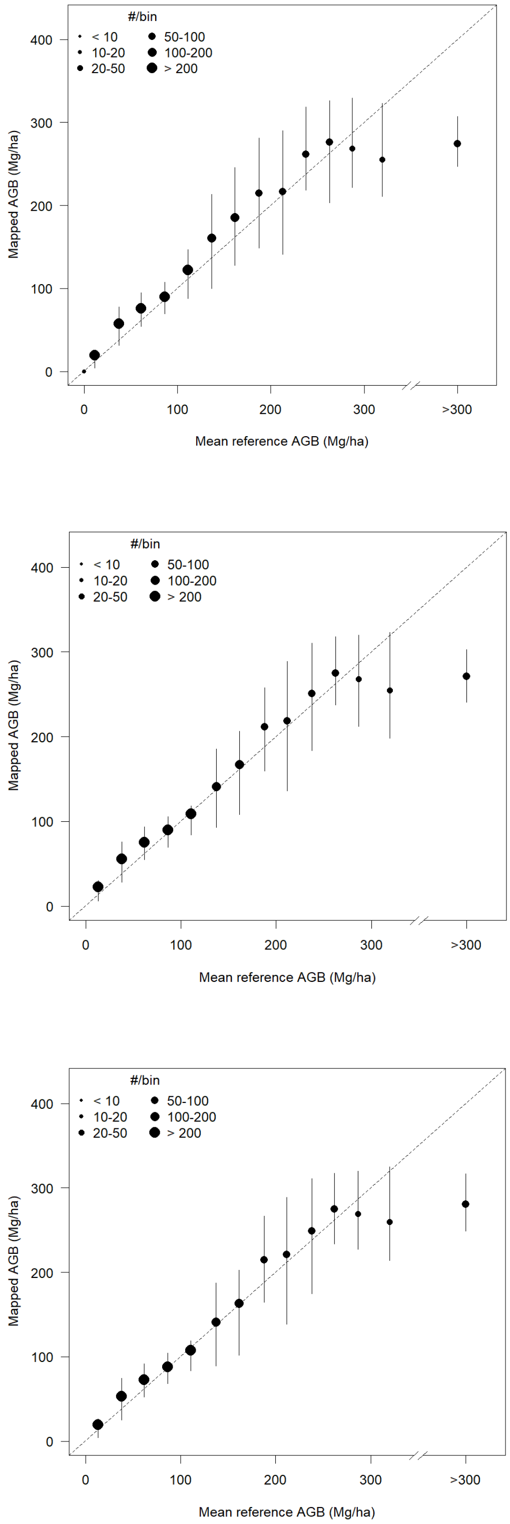

Figure 5. AGBref - AGBmap comparisons for Tier 1 data spatially aggregated to 0.1° and binned over 25 Mg/ha wide biomass ranges with whiskers representing the interquartile range of mapped biomass values and symbol size representing the number of 0.1° cells per biomass range. AGBref > 350 Mg/ha data are grouped into a single bin.

Table 13. Validation results per biomass range for Tier 1 data spatially aggregated to 0.1° cells for the 2017 map.

AGB_{ref} bin [Mg/ha]	# cells count	AGB_{ref}	AGB_{map}	*MD*	*RMSD*
		---------------------[Mg/ha] ---------------------			
0-50	1913	27	41	14	30
50-100	1512	71	81	10	32
100-150	505	120	120	0	52
150-200	208	172	184	13	74
200-250	119	224	234	10	91
250-300	110	273	272	-1	72
300-400	61	337	264	-73	114
>400	53	695	266	-429	505
total	4481	82	86	4	70

Table 14. Validation results per biomass range for Tier 1 data spatially aggregated to 0.1° cells for the 2018 map.

AGB_{ref} bin [Mg/ha]	# cells count	AGB_{ref}	AGB_{map}	*MD*	*RMSD*
		---------------------[Mg/ha] ---------------------			
0-50	1893	27	38	11	29
50-100	1524	71	79	8	32
100-150	512	120	119	-1	55
150-200	206	172	183	12	77
200-250	119	224	235	10	96
250-300	111	273	272	0	73
300-400	60	337	270	-67	112
>400	53	695	277	-418	495
total	4478	83	85	2	69

3.3. Comparisons with LiDAR-based, 1-km pixel Congo basin Forests AGB and EMAP 25-km aggregates

The results of the global AGM_{map} - AGB_{ref} comparisons at 0.1° resolution using LiDAR-based and CoFor AGB as reference data are shown in Figure 6 and Tables 15-17. The key observation, common to all three AGB maps, is map overestimation uniformly observed until 300 Mg/ha. This was not observed in the previous CCI map version, which suggests the current CCI maps underwent key modifications of the biomass retrieval algorithm in the wet tropics. Map underestimation is observed only beyond 320 Mg/ha. This effect may be influenced by the CoFor data having a dense plot network in the forest management areas of the Congo Basin. Since the original plot data inside the 1-km aggregates of the CoFor dataset are unavailable, we were unable to account for partly deforested areas. Such areas are likely to exist given the active forestry activities in the area. On the other hand, similar results were observed using the plot data (Tier 2 plots in particular), which builds confidence in using LiDAR and CoFor data for accuracy assessments.

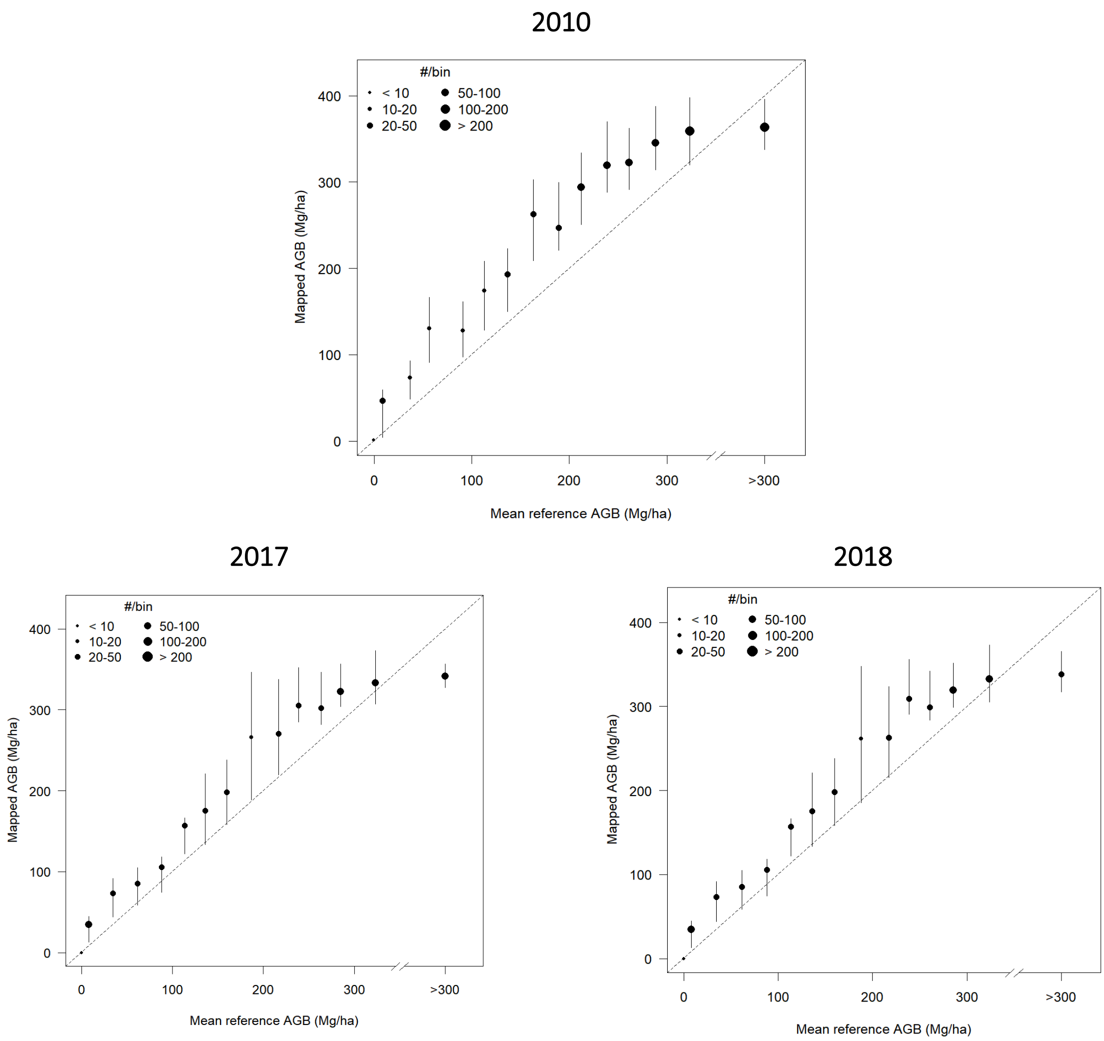

Figure 6. AGBref - AGBmap comparisons for LiDAR-based and CoFor AGB data spatially aggregated to 0.1° and binned over 25 Mg/ha wide biomass ranges with whiskers representing the interquartile range of mapped biomass values and symbol size representing the number of 0.1° cells per biomass range. AGBref > 350 Mg/ha data are grouped into a single bin.

Table 15. Validation results per biomass range using LiDAR-based and CoFor AGB data spatially aggregated to 0.1° cells for the 2010 map.

AGB_{ref} bin	# cells	AGB_{ref}	AGB_{map}	*MD*	*RMSD*
[Mg/ha]	count	--------------------[Mg/ha] --------------------			
0-50	64	15	49	34	61
50-100	25	74	129	55	78
100-150	35	130	188	58	80
150-200	51	178	254	76	105
200-250	122	226	307	81	104
250-300	176	275	334	59	82
300-400	279	340	363	23	61
>400	47	439	350	-89	125
total	799	260	300	40	83

Table 16. Validation results per biomass range using LiDAR-based and CoFor AGB data spatially aggregated to 0.1° cells for the 2017 map.

AGB_{ref} bin	# cells	AGB_{ref}	AGB_{map}	*MD*	*RMSD*
[Mg/ha]	count	--------------------[Mg/ha] --------------------			
0-50	127	13	41	28	44
50-100	40	75	95	21	48
100-150	46	125	166	41	68
150-200	43	169	222	53	92
200-250	68	231	292	62	96
250-300	93	276	314	38	71
300-400	125	336	336	0	58
>400	15	440	340	-100	114
total	557	193	220	26	69

Table 17. Validation results per biomass range using LiDAR-based and CoFor AGB data spatially aggregated to 0.1° cells for the 2018 map

AGB_{ref} bin	# cells	AGB_{ref}	AGB_{map}	*MD*	*RMSD*
[Mg/ha]	count	---------------------[Mg/ha]			---------------------
0-50	127	13	41	28	44
50-100	40	75	95	21	48
100-150	46	126	166	41	68
150-200	42	169	219	50	90
200-250	60	231	292	61	98
250-300	95	276	311	36	69
300-400	114	334	334	0	60
>400	7	448	342	-107	129
total	531	186	214	28	68

The 0.25° results using the EMAP dataset as reference data are shown in Figure **7** and Tables Table 18Table 19. Both 2017 and 2018 maps overestimate until AGB_{ref} ≈ 100 Mg/ha. Beyond this AGB value, map underestimation is observed. Note that fewer reference data are available as AGB increases.

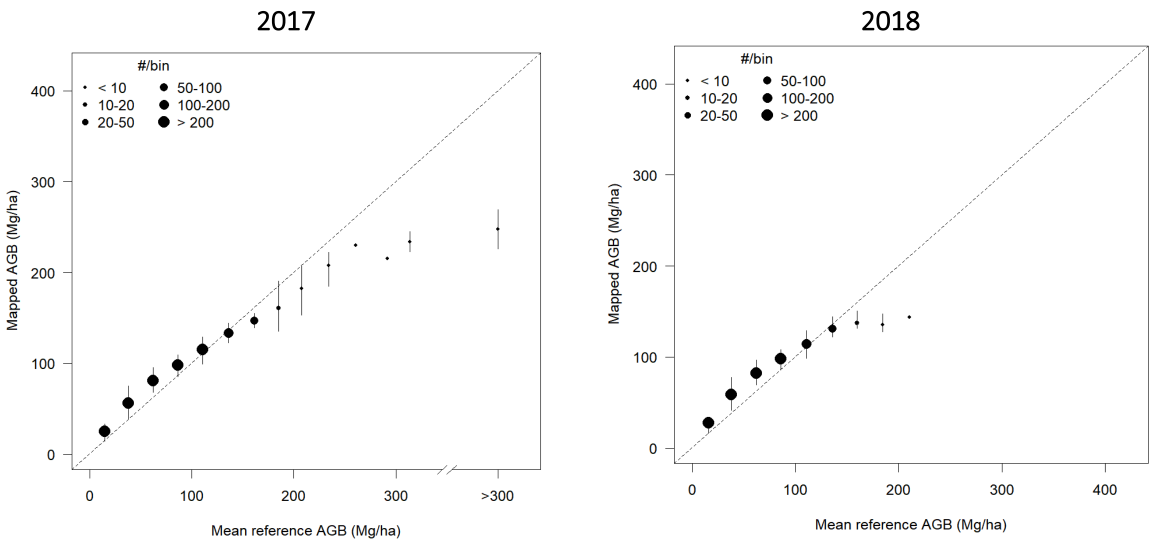

Figure 7. AGBref - AGBmap comparisons for LiDAR-based and EMAP AGB data spatially aggregated to 0.25° and binned over 25 Mg/ha wide biomass ranges with whiskers representing the interquartile range of mapped biomass values and symbol size representing the number of 0.25° cells per biomass range. AGBref > 350 Mg/ha data are grouped into a single bin.

Table 18. Validation results per biomass range using EMAP AGB data spatially aggregated to 0.25° cells for the 2017 map.

AGB_{ref} bin [Mg/ha]	# cells count	AGB_{ref}	AGB_{map}	MD	$RMSD$
		[Mg/ha]			
0-50	1617	28	43	15	24
50-100	1691	73	89	16	27
100-150	481	119	121	2	23
150-200	67	167	150	-17	32
200-250	12	225	200	-26	50
250-300	2	276	223	-54	58
300-400	4	339	241	-98	107
>400	3874	62	75	13	25
total	1617	28	43	15	24

Table 19. Validation results per biomass range using EMAP AGB data spatially aggregated to 0.25° cells for the 2018 map.

AGB_{ref} bin [Mg/ha]	# cells count	AGB_{ref}	AGB_{map}	MD	$RMSD$
		[Mg/ha]			
0-50	832	29	46	17	26
50-100	1010	73	90	16	27
100-150	252	117	119	2	22
150-200	23	166	137	-30	42
200-250	1	210	143	-67	67
250-300	2118	62	77	14	26
300-400	832	29	46	17	26
>400	1010	73	90	16	27
total	252	117	119	2	22

3.4. Summary tables on Tier 1-3 comparisons

To facilitate interpretation, the bias and RMSD estimates per map for different AGB_{ref} bins differentiated by Tier are shown in Table 20 and Table 21, respectively. Figure 8 provides the legend for the colour schemes used in these tables.

Table 20 shows that for the mid-range of AGB_{ref}, bias is within 20% of AGB_{ref} for Tier 1 data (which is consistent with GCOS requirements (GCOS, 2015)) but not for Tier 2 or 3 data. For the range between 250 and 400 Mg/ha the bias is usually less than 40% (in fact within 30%) of $AGB_{ref.}$ At the lower and upper ends of the AGB range considered, bias always exceeds 20%. The RMSD exceeds 20% in all cases except for Tier 3 in 2017 and 2018 when AGB_{ref} exceeds 250-300 Mg/ha (Table 21).

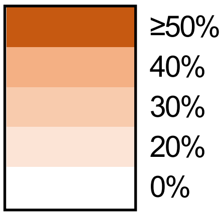

Figure 8. Legend for colour schemes used in summary tables of bias and RMSD.

Table 20. AGB bias [Mg/ha] differentiated per Tier and per AGB bin. Colour shading is based on relative bias; legend in Figure 7.

	---- Original resolution ----									0.1° cells Tier 1		
AGB bin	Tier 1			Tier 2			Tier 3					
	2010	2017	2018	2010	2017	2018	2010	2017	2018	2010	2017	2018
0-50	27	35	32	50	22	28	-	-	-	13	14	11
50-100	19	21	19	79	26	42	-	-	-	11	10	8
100-150	4	3	1	75	53	66	233	-	-	16	0	-1
150-200	-12	-12	-15	79	50	64		175	195	25	13	12
200-250	-34	-31	-34	58	67	67	67	73	82	14	10	10
250-300	-53	-54	-56	60	64	56	-101	0	-27	1	-1	0
300-400	-94	-92	-93	-31	-21	-23	-19	-15	-44	-77	-73	-67
>400	-484	-491	-489	-283	-256	-303	-198	-66	-57	-415	-429	-418

Table 21. Root mean square difference (RMSD) differentiated per Tier and per AGB bin.

	---- Original resolution ----									0.1° cells Tier 1		
	Tier 1			Tier 2			Tier 3					
	2010	2017	2018	2010	2017	2018	2010	2017	2018	2010	2017	2018
0-50	58	61	60	113	73	82	-	-	-	30	30	29
50-100	66	64	65	137	97	110		-	-	34	32	32
100-150	78	74	74	119	103	107	233	-	-	70	52	55
150-200	96	86	88	132	106	108	-	175	195	84	74	77
200-250	114	102	105	128	123	111	118	118	125	88	91	96
250-300	127	115	119	137	113	103	136	14	31	76	72	73
300-400	153	139	141	134	99	96	74	34	53	113	114	112
>400	832	848	846	381	374	416	215	72	63	497	505	495

3.5. Assessments by ecoregion

To allow assessments of validation results over different ecoregions, spatially aggregated comparisons of AGB_{ref} and AGB_{map} were stratified by biomes (Dinerstein et al., 2017). Results are presented in Figures Figure **9.** Comparisons between AGBref and the **2010** AGB map per biome (Dinerstein et al., 2017) using all available data binned over 25 Mg/ha wide biomass ranges with whiskers representing the interquartile range of mapped biomass values and symbol size representing the number of 0.1° cells per biomass range.Figure **11.** Comparisons between AGBref and the **2018** AGB map per biome (Dinerstein et al., 2017) using all available data binned over 25 Mg/ha wide biomass ranges with whiskers representing the interquartile range of mapped biomass values and symbol size representing the number of 0.1° cells per biomass range. and in Appendix B. Several strata had limited data or no data at all (e.g., deserts, flooded grassland, etc.). These cases are not included here.

For the boreal forests, mangroves, Mediterranean forest, woodland and scrub, and tundra biomes, reasonable fits with minor over-predictions are found in the lower AGB ranges. Map over- and under-prediction are mostly present in tropical and subtropical dry broadleaf forest. Note that data in the dry tropical regions are limited, which hampers drawing solid conclusions. Spikes of map over-prediction are also found in tropical and subtropical grasslands as well as in Mediterranean forests, woodland and scrub at around the 200Mg/ha bin. The AGB_{ref} density at which under-prediction starts differs by biome. For boreal forests and tundra, saturation of AGB_{map} occurs at approximately 100 Mg/ha, for example. The strong similarity of results for the temperate broadleaf and mixed forests biome (Figures 9-11) with those of the spatially aggregated results obtained with the Tier 1 data (Figure 5) was already mentioned above. Such similarity is also present between results from tropical and subtropical moist broadleaf forest and results from Tier 2 and LiDAR/CoFor.

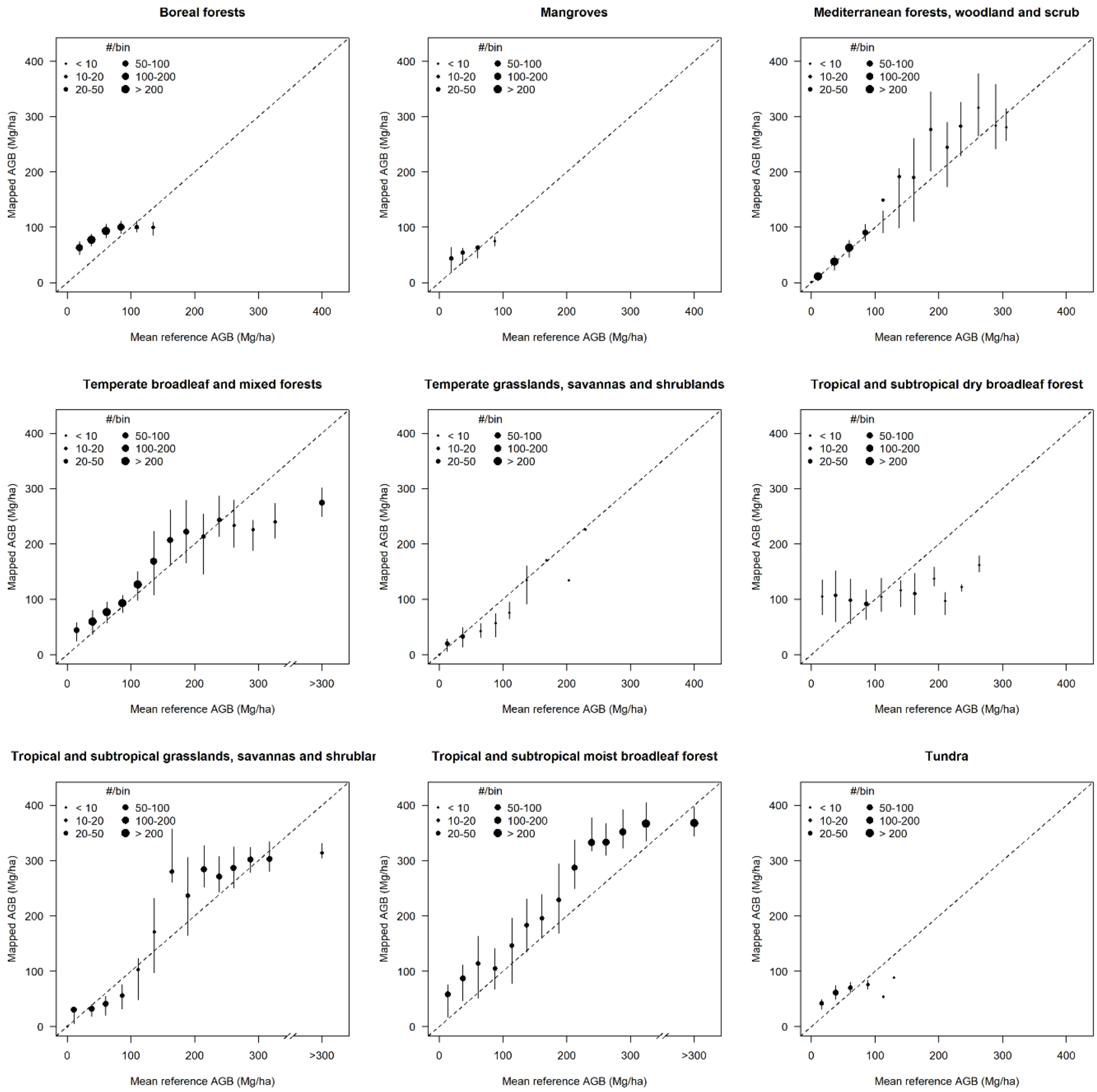

Figure 9. Comparisons between AGB$_{ref}$ and the **2010** AGB map per biome (Dinerstein et al., 2017) using all available data binned over 25 Mg/ha wide biomass ranges with whiskers representing the interquartile range of mapped biomass values and symbol size representing the number of 0.1° cells per biomass range.

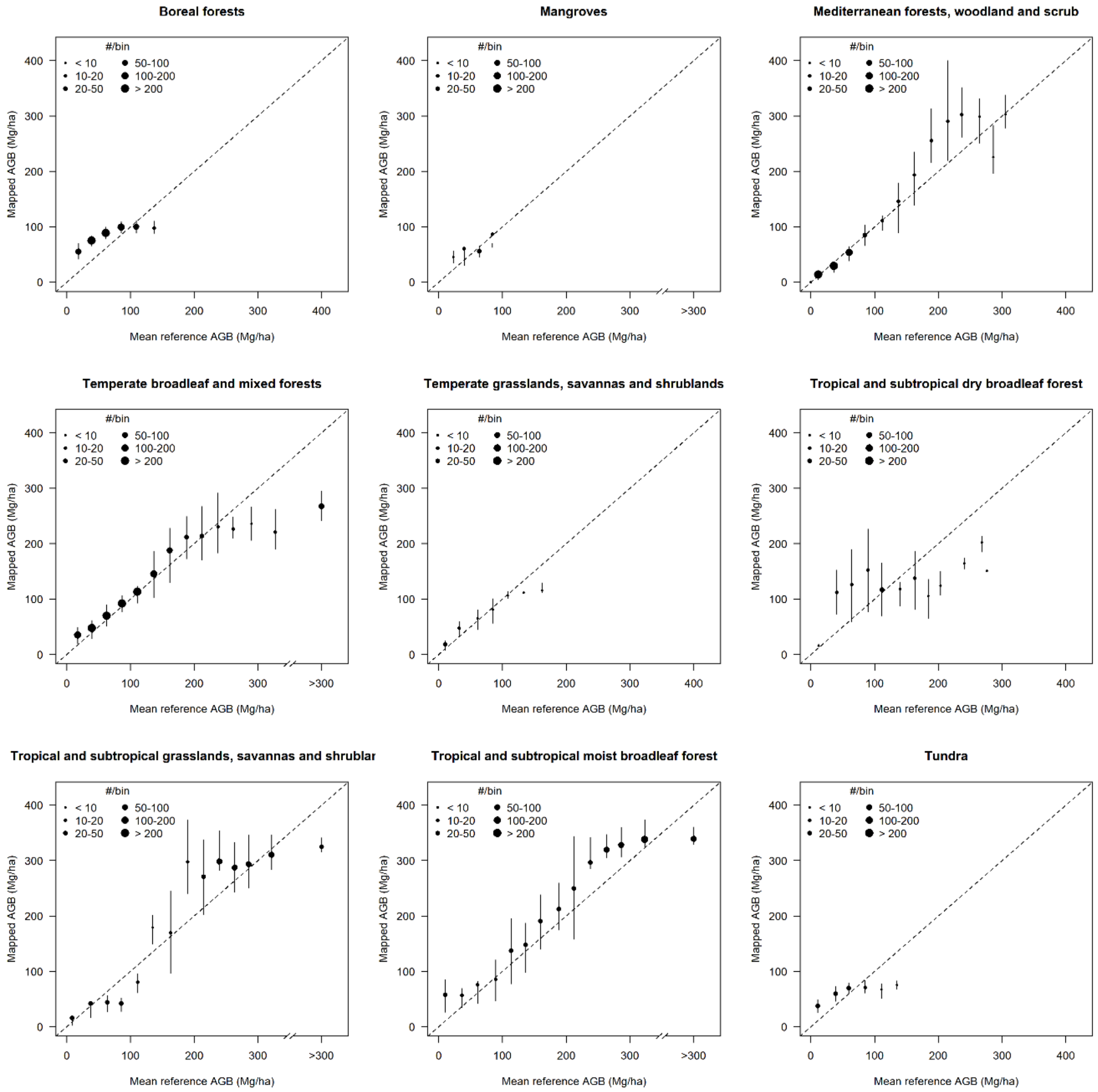

Figure 10. Comparisons between AGB_{ref} and the **2017** AGB map per biome (Dinerstein et al., 2017) using all available data binned over 25 Mg/ha wide biomass ranges with whiskers representing the interquartile range of mapped biomass values and symbol size representing the number of 0.1° cells per biomass range.

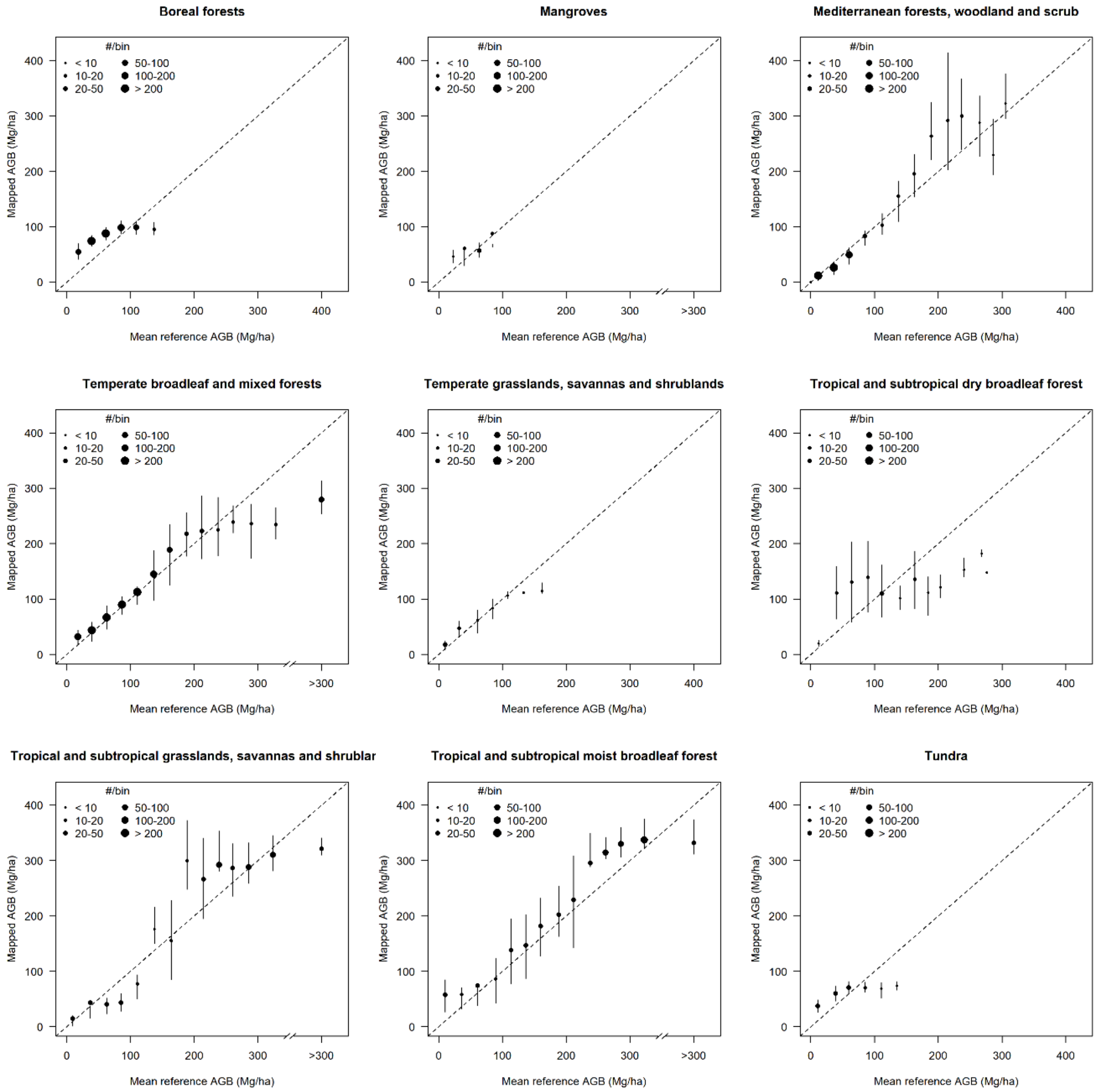

Figure 11. Comparisons between AGB_{ref} and the **2018** AGB map per biome (Dinerstein et al., 2017) using all available data binned over 25 Mg/ha wide biomass ranges with whiskers representing the interquartile range of mapped biomass values and symbol size representing the number of 0.1° cells per biomass range.

3.6. User-led validation

Two recent user-led independent map validations using own country data are reported here. First, the Wales NFI (1600 plots) was used and compared with the CCI Biomass map of 2017 by Forest Research in conjunction with Living Wales (Planque et al., 2021) using the *plot-to-map* online tool (see PVP for information about the tool). The Russian Forest Federal Agency has also facilitated the use of 10,000 Russian NFI plots as part of an effort to update the carbon stocks of Russia (Schepaschenko et al., 2021). The Russian data allowed comparisons of Growing Stock Volumes (GSVs) instead of AGB. GSV from the NFI was compared with the GSV map rom which the CCI Biomass 2017 map originated.

The comparisons in Figures Figure 12Figure 13 and Table 22 concerning the two country cases agree with the earlier results (Figures 11-13) where the most agreement between plot data and CCI maps were found for the intermediate AGB ranges.

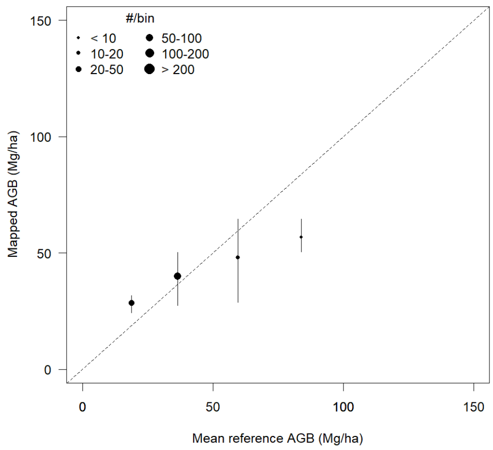

Figure 12. AGBref - AGBmap comparisons for 1600 NFI plots of Wales spatially aggregated to 0.1° and binned over 25 Mg/ha wide biomass ranges with whiskers representing the interquartile range of mapped biomass values and symbol size representing the number of 0.1° cells per biomass range. AGBref > 350 Mg/ha data are grouped into a single bin.

Table 22. Validation results per biomass range using AGB data of Wales NFI spatially aggregated to 0.1° cells for the 2017 map.

AGB_{ref} bin	# cells	AGB_{ref}	AGB_{map}	*MD*	*RMSD*
[Mg/ha]	count	---------------------[Mg/ha]	---------------------		
0-50	832	29	46	17	26
50-100	1010	73	90	16	27
total	252	117	119	2	22

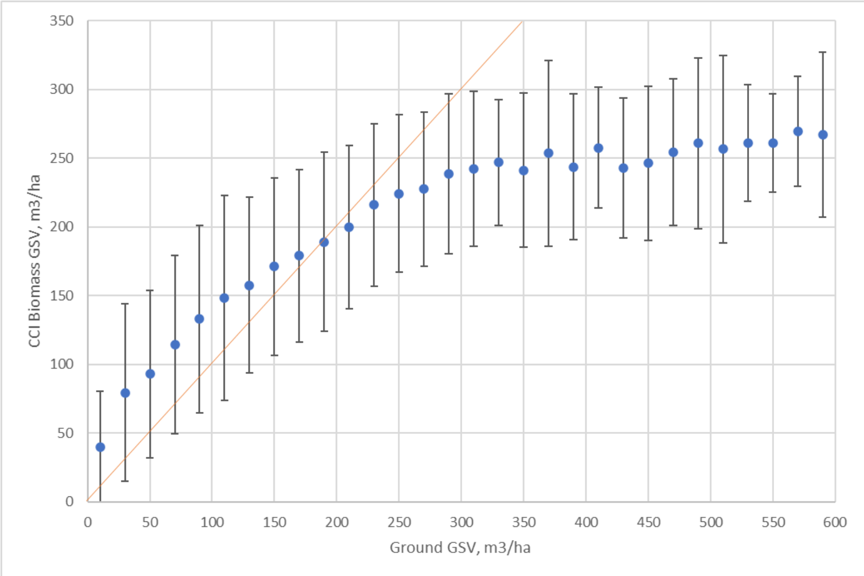

Figure 13. GSVref - GSVmap comparisons for the Russian NFI averaged every 20 m^3/ha (Schepaschenko et al., 2021).

3.7. Summary tables of the assessments by ecoregion

To facilitate interpretation per AGB map, the bias and RMSD estimates for different AGB$_{ref}$ bins differentiated by biome are shown in Table 23. AGB bias [Mg/ha] differentiated per biome and per AGB bin for the 2010 map. Colour shading is based the legend shown in Figure 7. Table 28.

The tables re-emphasize our overall finding that in the lower and higher AGB ranges the bias and RMSD are larger than for the mid-ranges. The bias for the mid-ranges for most biomes is around or below 20%, while the RMSD is above 20%.

The quantity of available reference information differs for different regions and there is lower confidence for some with limited reference data, including the (sub-)tropical dry forests and grasslands, mangroves, temperate grasslands and tundra.

Table 23. AGB bias [Mg/ha] differentiated per biome and per AGB bin for the 2010 map. Colour shading is based the legend shown in Figure 7.

AGB_{ref} [Mg/ha]	Boreal	Mangrove	Mediterranean	Temperate broadleaf/mixed	Temperate grasslands, savannas and shrublands	Tropical/subtropical dry broadleaf	tropical and subtropical grasslands	Tropical and subtropical moist broadleaf forest	Tundra
0-50	32	20	1	22	3	76	4	48	23
50-100	16	1	4	11	-28	20	-23	37	1
100-150	40		46	22	-25	-15	10	41	-56
150-200	-		58	41	2	-53	73	39	
200-250	-		40	2	-36	-113	52	86	
250-300	-		36	-46		-102	20	67	
300-400	-		-25	-103			-21	26	
>400	-			-399			-136	-75	
Total	27	13	3	3	-6	6	12	40	13

Table 24. Root mean square difference (RMSD) differentiated per biome and per AGB bin for the 2010 map. Colour shading is based on the legend shown in Figure 7; column headings are as above.

0-50	43	41	12	35	18	92	36	75	28
50-100	33	36	24	31	35	50	37	75	19
100-150	25		129	63	50	44	70	86	57
150-200			115	76	2	69	123	92	
200-250	-		99	63	49	115	83	114	
250-300	-		99	73		104	55	89	
300-400	-		55	117			63	64	
>400	-			483			151	101	
Total	38	39	26	95	27	70	66	84	28

Table 25. AGB bias [Mg/ha] differentiated per biome and per AGB bin for the 2017 map. Colour shading is based on the legend shown in Figure 7.

AGB_{ref} [Mg/ha]	Boreal	Mangrove	Mediterranean	Temperate broadleaf/mixed	Temperate grasslands, savannas and shrublands	Tropical/subtropical dry broadleaf	tropical and subtropical grasslands	Tropical and subtropical moist broadleaf forest	Tundra
0-50	36	21	-1	11	10	63	6	39	19
50-100	23	-4	-6	6	-1	62	-30	6	2
100-150	-15		4	4	-7	0	-2	18	-47
150-200			44	25	-47	-35	59	29	
200-250	-		72	-1		-78	58	50	
250-300	-		-6	-42		-81	15	48	
300-400	-		-2	-106			-18	0	
>400	-			-430			-161	-116	
Total	25	5	2	-7	5	11	10	20	6

Table 26. Root mean square difference (RMSD) differentiated per biome and per AGB bin for the 2017 map. Colour shading is based on the legend shown in Figure 7; column headings are as above.

0-50	39	56	15	28	18	83	52	60	23
50-100	29	39	24	27	26	95	37	53	18
100-150	26		56	49	16	51	56	74	52
150-200			96	67	49	65	122	81	
200-250	-		117	68		82	103	99	
250-300	-		85	66		88	68	76	
300-400	-		51	118			68	65	
>400	-			507			177	143	
Total	33	46	31	96	22	75	77	79	25

Table 27. AGB bias [Mg/ha] differentiated per biome and per AGB bin for the 2018 map. Colour shading is based on the legend shown in Figure 7.

AGB_{ref} [Mg/ha]	Boreal	Mangrove	Mediterranean	Temperate broadleaf/mixed	Temperate grasslands, savannas and shrublands	Tropical/subtropical dry broadleaf	tropical and subtropical grasslands	Tropical and subtropical moist broadleaf forest	Tundra
0-50	35	21	-3	7	10	62	6	40	23
50-100	22	-3	-9	3	-1	59	-31	6	4
100-150	-15		6	4	-7	-10	-7	17	-46
150-200			49	28	-48	-35	50	19	
200-250	-		72	2		-85	53	43	
250-300	-		-11	-35		-97	13	47	
300-400	-		17	-93			-21	3	
>400	-			-418			-172	-146	
Total	25	5	-1	-8	4	6	5	22	11

Table 28. Root mean square difference (RMSD) differentiated per biome and per AGB bin for the 2018 map. Colour shading is based on the legend shown in Figure 7; column headings are as above.

0-50	39	57	15	27	18	82	53	60	29
50-100	29	42	24	29	26	93	38	54	21
100-150	28		54	52	16	50	59	73	53
150-200			99	73	51	65	119	76	
200-250	-		126	76		90	102	96	
250-300	-		92	68		99	66	73	
300-400	-		77	109			69	69	
>400	-			497			184	184	
Total	33	46	32	95	22	75	75	78	29

3.8. AGB map intercomparison

In this section we assess the stability of map error among the current (version 3) three CCI-Biomass AGB products and compare the most recent 2010 and 2017 versions with the version 2 products.

Stability of $AGB_{map} – AGB_{ref}$ differences among the 2010, 2017 and 2018 AGB products

According to the World Meteorological Organization (2011) the user requirement for stability is in general a requirement on the extent to which the error of a product remains constant over a longer period. To assess stability of plot-map differences over the three epochs, Figure 14 shows AGB residuals between harmonized Tier 1-3 plot data and mapped AGB aggregated to the 0.1° cell level for each combination of map reference years. Whilst the residuals in 2017 are very similar to those in 2018 (bottom row), the 2010 map has many cells for which the residuals differ substantially from those in 2017 and 2018, as can be observed in the top row of Figure 14.

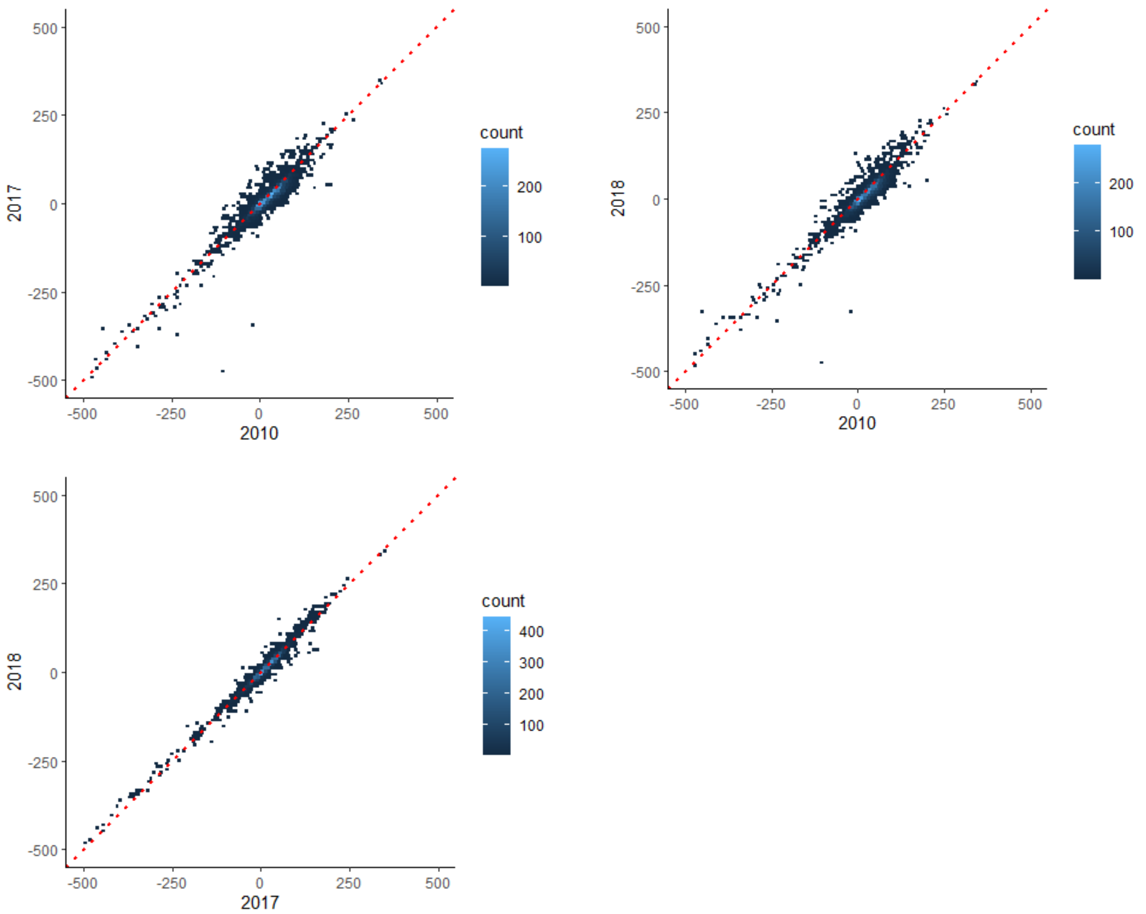

Figure 14. AGB residuals between harmonized Tier1-3 plot data and mapped AGB at 0.1° cell level for each combination of map reference years. The red dashed line is the 1:1 line.

The map producer may want to know where the largest instabilities in the residuals occur. Such information is provided in Figure 15 where the locations of the 5% most negative differences between the 2010 and 2017 products (2010 – 2017; i.e., points above the 1:1 diagonal in Figure 14) are plotted as red circles whilst the 5% largest positive differences (i.e., points below the 1:1 diagonal) are shown by blue crosses. Several sites have entirely either large positive or large negative differences, but in other places, such as east Australia, Madagascar, the northern Balkans and Mexico (Yucatán), both extremes occur close to one another. Figure 16 is a virtually identical figure showing the locations of cells with the most extreme differences between 2010 and 2018 residuals while Figure 17 does so for the 2017 and 2018 residuals. The latter figure has a different pattern of highs and lows but, with additional nearby occurrences of extremes in Gabon.

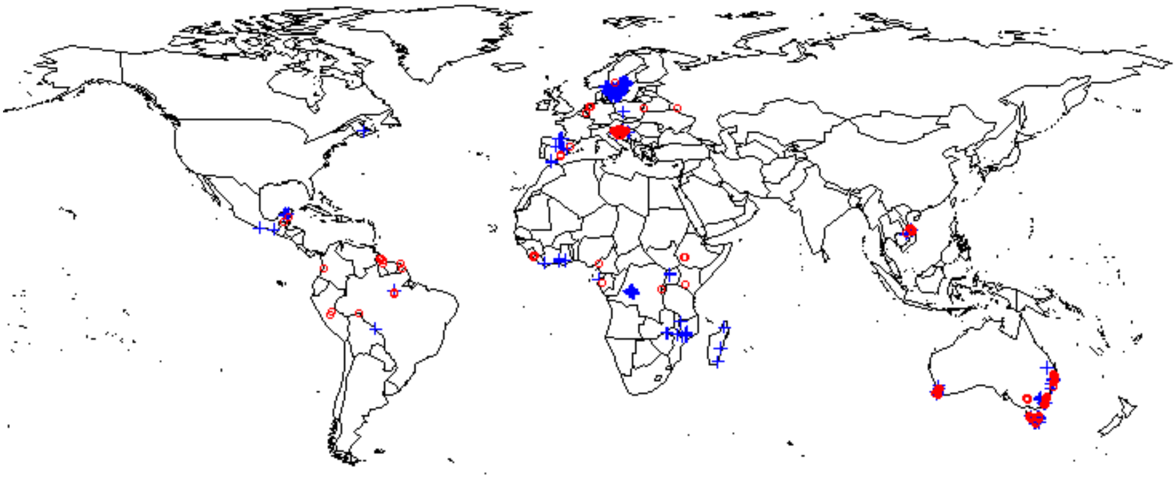

Figure 15. Locations of 0.1° cells with the most extreme differences between residuals in the 2010 and 2017 AGB products (2010 – 2017). The 5% cells with the most negative differences (i.e., 2017 > 2010) are indicated in red whilst the 5% largest positive differences (i.e., 2017 < 2010) are shown in blue.

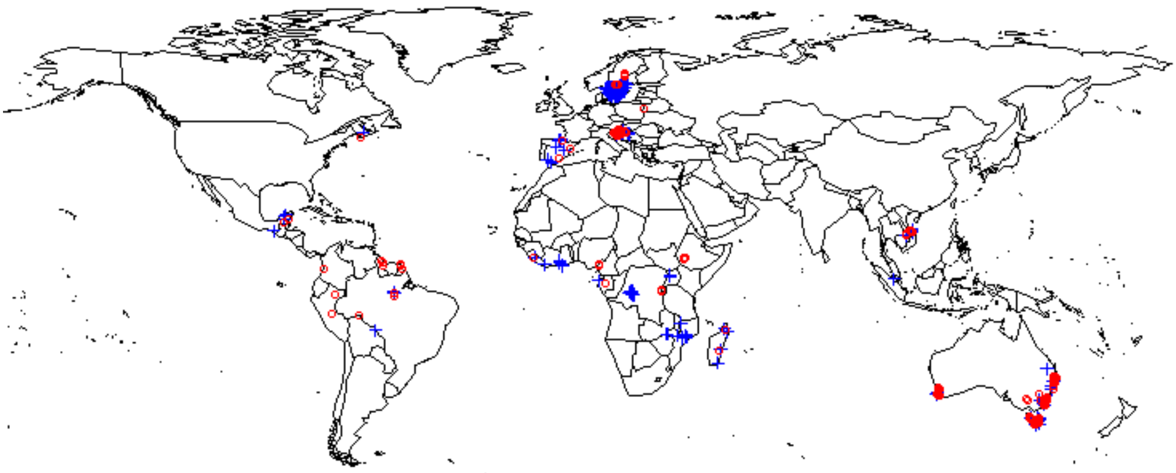

Figure 16. Locations of 0.1° cells with the most extreme differences between residuals in the 2010 and 2018 AGB products (2010 – 2018). The 5% cells with the most negative differences (i.e., 2018 > 2010) are indicated in red whilst the 5% largest positive differences (i.e., 2018 < 2010) are shown in blue.

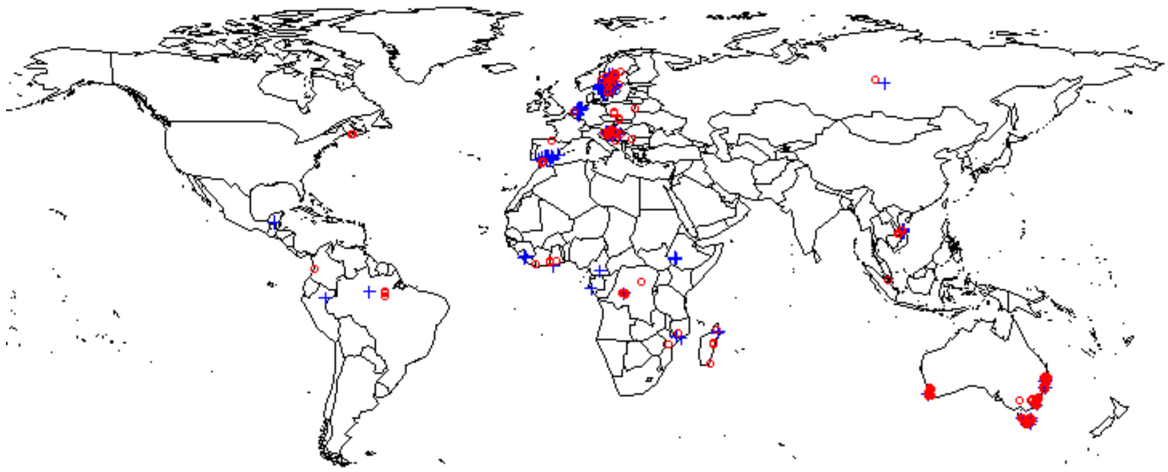

Figure 17. Locations of 0.1° cells with the most extreme differences between residuals in the 2017 and 2018 AGB products (2017 – 2018). The 5% cells with the most negative differences (i.e., 2018 > 2017) are indicated in red whilst the 5% largest positive differences (i.e., 2018 < 2017) are shown in blue.

Comparison of current maps with previous 2010, 2017 and 2018 AGB products

Figure 18 shows the global AGB_{map} - AGB_{ref} comparisons spatially aggregated to 0.1° and binned over 25 Mg/ha wide biomass ranges for CCI Biomass versions 2 and 3 in three epochs. In most AGB bins, map bias for the newer CCI maps version has decreased except for > 350 Mg/ha. As mentioned before, this bias arises from a set of plots in southern Australia, where the current map estimates are reduced (not shown here).

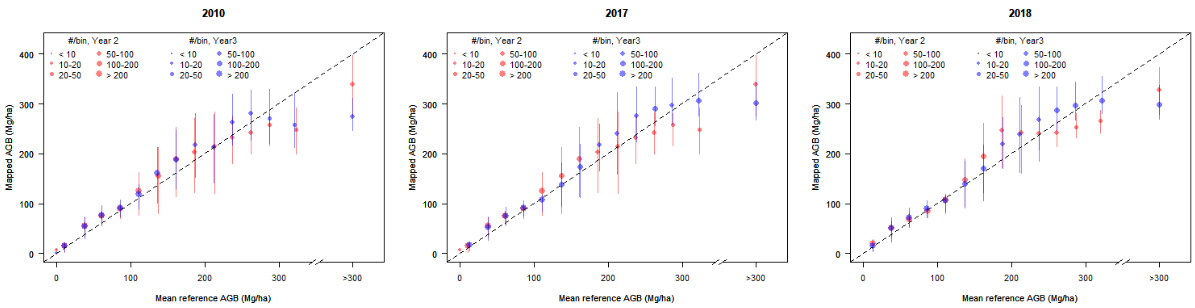

Figure 18. Global AGB_{map} - AGB_{ref} comparisons based on inverse variance weighted Tier 1-3 plot data spatially aggregated to 0.1° cells.

3.9. Within-pixel sampling error

Using the forest only LiDAR-derived AGB data from forest sites in Remningstorp, Sweden (Ulander et al., 2011), and Lope, Gabon (Hajnsek et al., 2017), the variograms shown in Figure 19 were estimated. The Remningstorp variogram was modelled by two exponential structures with partial sills of 3579 and 1899 Mg^2/ha^2 and range parameters of 95 and 531 m, respectively. The Lope variogram was modelled by a 4053 Mg^2/ha^2 nugget and a single exponential structure with partial sill of 10553 Mg^2/ha^2 and a range parameter of 85 m. Note that the effective range of an exponential variogram is approximately three times the range parameter.

Not surprisingly, the tropical high biomass Lope site has much larger short-range spatial variation than the boreal Remningstorp site (note the different scales on the y-axes).

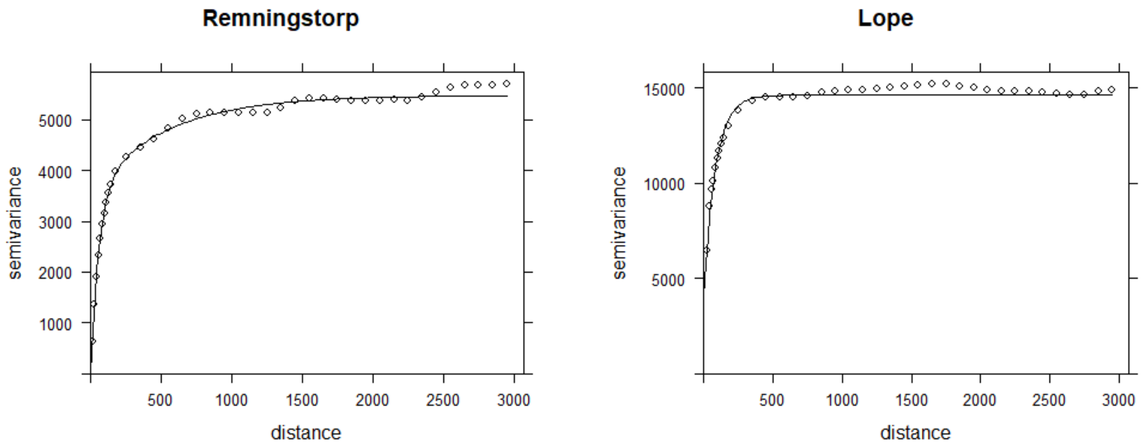

Figure 19. Variograms for the Remningstorp and Lope forest sites. Open dots indicate the experimental variogram and the solid lines represent the fitted models.

Based on the variograms, and assuming single plots with the size of the LiDAR footprints (i.e., 0.01 ha for Remningstorp and 0.04 ha for Lope) centred in 1 ha AGB map pixels, the variance of the plots was found to be 1421 and 6714 Mg^2/ha^2 for the two sites. Hence, the standard deviations amount to 38 and 82 Mg/ha, respectively, which is not negligible.

As demonstrated in the PUG (Santoro, 2020), within-pixel sampling error may suggest map bias even if the map provides a perfect representation of mean AGB at 1 ha spatial support. To replicate this issue using a geostatistical approach, Figure 20 shows a scatterplot of 0.04 ha plot AGB values on the x-axis centred and conditioned on 1 ha pixels that are plotted on the y-axis. The pixel values are in the range 10 to 400 Mg/ha and the plot values are drawn from Gaussian populations with mean given by the pixel value and variance and spatial correlation given by the Lope variogram. Any negative value drawn from a Gaussian population was set to zero.

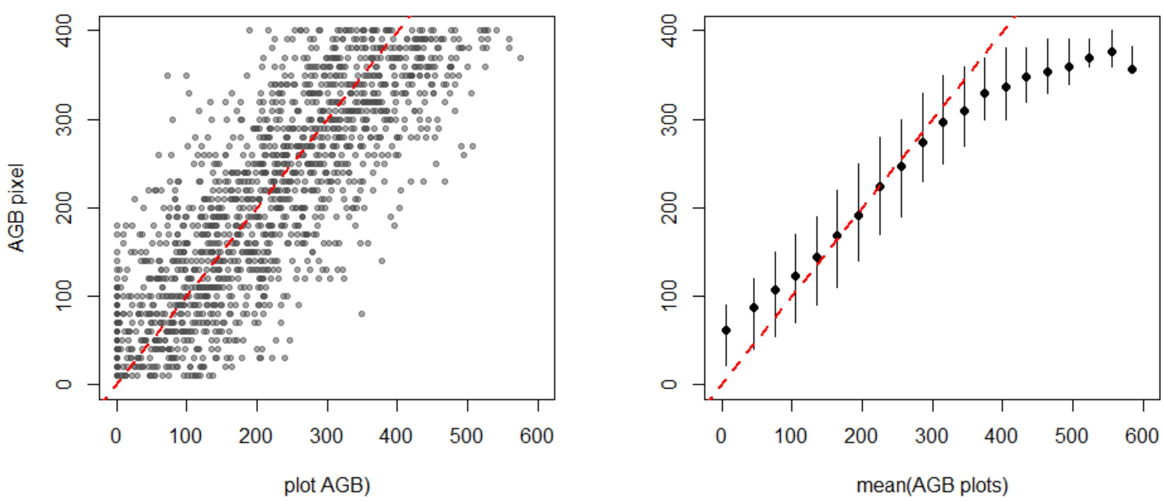

Figure 20. Scatterplot of 0.04 ha plot values conditioned on 1 ha pixel values (left) and binned over 30 Mg/ha wide biomass ranges with dots representing mean AGB and whiskers representing the interquartile range of pixel biomass values for plots inside the bins (right). The dashed red lines are 1:1 lines.

The scatterplot and the interquartile whisker plot in Figure 20 suggest the pixel overestimates low AGB and underestimates high AGB at plot level. However, the plot data were conditioned on the pixel data. Therefore, the observed effect is entirely due to the within-pixel sampling error.

The above effect reduces substantially if multiple plots are used to represent a pixel. To demonstrate this, the above experiment was repeated with five plots regularly spread over the pixel. In Figure 21, the means of the AGB from five plots are on the x-axis, while the conditioning pixel values are on the y-axis. In this figure, the bias observed in Figure 20 is mostly absent, except for the far ends of the AGB range.

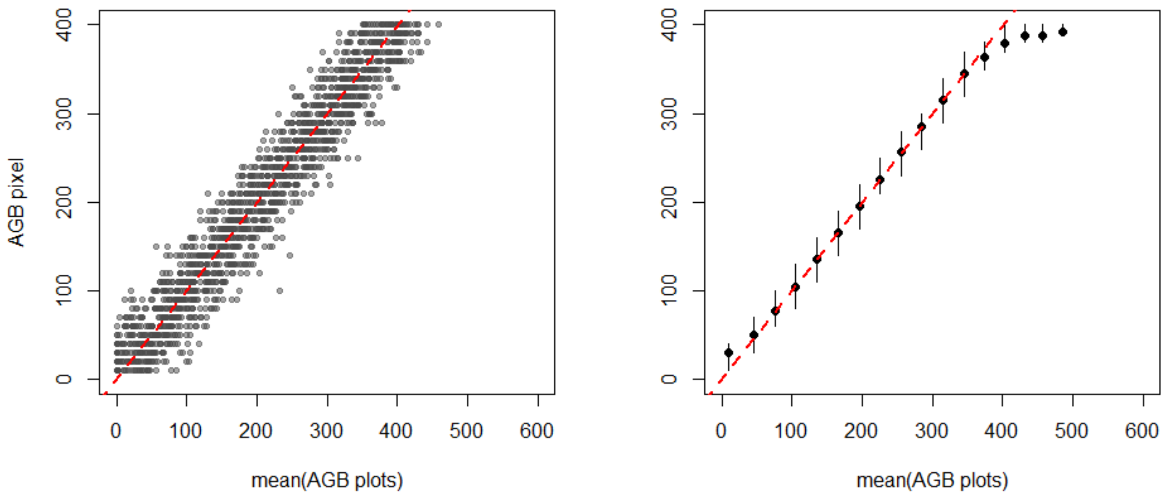

Figure 21. Scatterplot of the mean of 0.04 ha plot values conditioned on 1 ha pixel values (left) and binned over 30 Mg/ha wide biomass ranges with dots representing mean AGB and whiskers representing the interquartile range of pixel biomass values (right). The dashed red lines are 1:1 lines.

The reasons for including this section in the PVIR are (1) to corroborate the experiment shown in the PUG (Santoro, 2020) and (2) to demonstrate a method for diagnosing the within-pixel sampling error and show the importance of taking it into account when validating map pixels with data from small plots. For the latter, we need variography for the different environmental circumstances (e.g., biomes), which can be obtained from small footprint (0.01-0.04 ha) LiDAR-derived AGB data , such as the data used in this section. Currently, we have such data only for a single boreal forest site and one site in a tropical forest. More data in these biomes as well as other biomes are needed to routinely account for the within-pixel sampling variance in AGB_{map} – AGB_{ref} comparisons.

Conclusions

Fully reported and transparent validation is important for increasing acceptance of satellite-derived products in the user community. To assess the accuracy of the AGB estimates of the new 2010, 2017 and 2018 CCI Biomass global maps, AGB predictions were compared with independent plot data, LiDAR-based AGB estimates and recently released CoFor and EMAP data, which were used as reference data.

The plot data were adjusted for temporal discrepancies and partial forest fraction (see PVP). Three Tiers of plot data were defined, ranging from a large set of data (70540 – 119744 plots, depending on the reference year of the AGB map) from small plots (on average 0.15 ha), including small NFI plots, to a small set of data from large (> 6 ha) research plots (21 – 27 plots). The latter Tier 3 data mainly consist of plots in the tropics that, though of high quality, are so few in number that they barely allow conclusions to be drawn about the quality of the CCI Biomass maps. Tier 2 plots (464 – 716 plots), with an average size of 1 ha, revealed that globally the CCI Biomass maps at their original 1 ha resolution tend to over-predict AGB_{ref} up to 300 Mg/ha and to under-predict AGB_{ref} beyond that. Similar results were found with the Tier 1 data, which builds confidence in using Tier 1 plot data for regional accuracy assessments. It should be noted that part of the observed underestimation of high biomass and overestimation of low biomass observed for small plots can be attributed to within-pixel sampling error that occurs because the AGB of single small plots may significantly differ from the population mean in the pixel.

Spatial aggregation of plot and map data to 0.1° cells (a level of aggregation suitable for most climate modellers) considerably improved the agreement between AGB_{ref} and AGB_{map}, though over-prediction was still observed in the low biomass range and higher reference biomass was under-predicted. Similar results were obtained with LiDAR-based AGB estimates and 1-km pixel Congo basin Forests AGB (CoFor) which suggests their suitability to serve as reference data for assessing global AGB products.

In general, between 50 Mg/ha and 400 Mg/ha, mean differences between AGB_{map} and AGB_{ref} were found to be well within 20% of AGB_{ref} at 0.1° cell level. This does not hold for the RMSD, which over the entire biomass range exceeds 20% of AGB_{ref} for the three maps. Nevertheless, it is concluded that spatial aggregation reduces the effect of localized AGB fluctuations in the map and plot-map geolocation mismatches. The AGB_{map} - AGB_{ref} comparisons at 0.1° resolution differentiated by biome (Dinerstein et al., 2017) produced patterns similar to the global comparison for many biomes and particularly highlighted confidence in the regional biomass estimations up to 300 Mg/ha for the different tropical forest regions. Fits between AGB_{ref} and AGB_{map} were worse for the tropical and subtropical *dry* broadleaf forest biome. Lack of access to a larger set of reference data for this biome may have affected this finding.

The overall analysis at 0.1° cell level revealed that version 3 of the CCI Biomass AGB maps provides better estimates of the high biomass range than previous versions. However, we observed overestimation of AGB within the tropics up to AGB_{ref} = 300 Mg/ha and underestimation beyond AGB_{ref} ≈ 350 Mg/ha, which was traced to a set of small plots in southeast Australia with widely different AGB densities.

Differences between AGB_{ref} and AGB_{map} were spatially similar in the 2017 and 2018 AGB products, but larger differences were found either of those two products and the 2010 AGB product. The locations of the largest differences were mapped to help identify potential reasons for their occurrence.

This PVIR demonstrated a geostatistical method for assessing the variance of within-pixel sampling error using variography derived from small footprint LiDAR-based AGB estimates from forest sites in Sweden and Gabon. Additional datasets are needed to extend this analysis and use it for error budgeting when using (small) plot data for AGB map assessment.

Acknowledgements

We are grateful to all data contributors (see Appendix A) for providing forest plot data for the independent validation of the CCI Biomass maps. We are also thankful to Forest Research (in conjunction with the European Regional Development Fund/Welsh Government funded Ser Cymru ‘Living Wales) and the Russian Forest Federal Agency in conjunction with the team of Dmitry Schepaschenko for the user-led independent validation using country data

References (including references from Appendix A)

Avitabile, V., Baccini, A., Friedl, M. A., & Schmullius, C. (2012). Capabilities and limitations of Landsat and land cover data for aboveground woody biomass estimation of Uganda. *Remote Sensing of Environment, 117*, 366-380. https://doi.org/10.1016/j.rse.2011.10.012.

Avitabile, V., Schultz, M., Herold, N., de Bruin, S., Pratihast, A. K., Manh, C. P., . . . Herold, M. (2016). Carbon emissions from land cover change in Central Vietnam. *Carbon Management, 7*(5-6), 333-346. doi:10.1080/17583004.2016.1254009

Brown, S., Gillespie, A. J. R., & Lugo, A. E. (1989). Biomass Estimation Methods for Tropical Forests with Applications to Forest Inventory Data. *Forest Science, 35*(4), 881-902. https://doi.org/10.1093/forestscience/35.4.881.

Carreiras, J. M. B., Vasconcelos, M. J., & Lucas, R. M. (2012). Understanding the relationship between aboveground biomass and ALOS PALSAR data in the forests of Guinea-Bissau (West Africa). *Remote Sensing of Environment, 121*, 426-442. https://doi.org/10.1016/j.rse.2012.02.012.

CEOS (2021). *Aboveground Woody Biomass Product Validation Good Practices Protocol, Version 1.0* (ed. Duncanson, L., Armston, J., Disney, M., Nickeson, J., Minor, D. & Camacho, F.)

Clark, D. B., & Clark, D. A. (2000). Landscape-scale variation in forest structure and biomass in a tropical rain forest. *Forest Ecology and Management, 137*(1), 185-198. https://doi.org/10.1016/S0378-1127(99)00327-8.

de Bruin, S., Herold, M., & Araza, A. (2019a). *CCI Biomass Product Validation Plan, Year 1, Version 1*. Retrieved from http://cci.esa.int/sites/default/files/biomass%20D2.5%20Product%20Validation%20Plan%20%28PVP%29%20V1.0.pdf.

de Bruin, S., Herold, M., & Araza, A. (2019b). CCI Biomass Product Validation & Intercomparison Report Year 1 Version 1.0. https://climate.esa.int/sites/default/files/biomass_D4.1_Product_Validation_%26_Intercomparison_Report_V1.1.pdf.

de Bruin, S., Herold, M., & Araza, A., Lucas, R. (2020). *CCI Biomass Product Validation Plan, Year 2, Version 2*. https://climate.esa.int/sites/default/files/Biomass_D2.5_Product_Validation_Plan_V2.0.pdf.

de Bruin, S., Herold, M., & Araza, A., Lucas, R. (2021). *CCI Biomass Product Validation Plan, Year 3, Version 3*. https://climate.esa.int/sites/default/files/Biomass_D2.5_Product_Validation_Plan_V3.0.pdf.

DeVries, B., Avitabile, V., Kooistra, L., & Herold, M. (2012). *Monitoring the impact of REDD+ implementation in the Unesco Kafa biosphere reserve, Ethiopia*. Paper presented at the Sensing a Changing World, Wageningen. http://www.wageningenur.nl/upload_mm/9/d/c/f80b6db7-9c3c-4957-8717-6fdc6e46e60f_deVries.pdf.

Dinerstein, E., Olson, D., Joshi, A., Vynne, C., Burgess, N. D., Wikramanayake, E.,Saleem, M. (2017). An Ecoregion-Based Approach to Protecting Half the Terrestrial Realm. *BioScience, 67*(6), 534-545. https://doi.org/10.1093/biosci/bix014.

GCOS (2015). *Status of the Global Observing System for Climate*, GCOS-195, WMO.

Hajnsek, I., Pardini, M., Jäger, M., Horn, R., Kim, J.S., Jörg, H., Papathanassiou, K., Dubois-Fernandez, P., Dupuis, X., Wasik, V. (2017). Technical Assistance for the Development of Airborne SAR and Geophysical Measurements During the AFRISAR Experiment. Final Report, Deliverable DD-4. pp. 152.

Hansen, M. C., Potapov, P. V., Moore, R., Hancher, M., Turubanova, S. A., Tyukavina, A., . . . Townshend, J. R. G. (2013). High-Resolution Global Maps of 21st-Century Forest Cover Change. *Science, 342*(6160), 850-853. https://doi.org/10.1126/science.1244693.

Hijmans, R. J. (2017). raster: Geographic Data Analysis and Modeling (Version 2.6). Retrieved from https://CRAN.R-project.org/package=raster.

Hirsh, F., Jourget, J. G., Feintrenie, L., Bayol, N., & Ebaá Atyi, R. (2013). *Projet pilote REDD+ de la Lukénie*. Retrieved from Bogor, Indonesia: https://agritrop.cirad.fr/572060/1/document_572060.pdf.

Horn, B. (1981). Hill shading and the reflectance map. *Proceedings of the IEEE, 69*, 14-47. doi:10.1109/PROC.1981.11918

IPPC. (2006). IPCC Guidelines for National Greenhouse Gas Inventories. https://www.ipcc.ch/report/2006-ipcc-guidelines-for-national-greenhouse-gas-inventories/

IPCC. (2019). 2019 Refinement to the 2006 IPCC Guidelines for National Greenhouse Gas Inventories. (table 4.9). https://www.ipcc.ch/report/2019-refinement-to-the-2006-ipcc-guidelines-for-national-greenhouse-gas-inventories/

Kyriakidis, P.C. (2004). A Geostatistical Framework for Area-to-Point Spatial Interpolation. *Geographical Analysis*, 36: 259-289. https://doi.org/10.1111/j.1538-4632.2004.tb01135.x.

Labrière, N., Tao, S., Chave, J., Scipal, K., Toan, T. L., Abernethy, K., . . . Saatchi, S. (2018). In SituReference Datasets From the TropiSAR and AfriSAR Campaigns in Support of Upcoming Spaceborne Biomass Missions. *IEEE Journal of Selected Topics in Applied Earth Observations and Remote Sensing, 11*(10), 3617-3627. doi:10.1109/JSTARS.2018.2851606

Labrière, N., & Chave, J. (2020a) CCI Biomass project – In situ datasets: Processing and validation of Sustainable Landscape Brazil data (CCI Biomass internal report).

Labrière, N., & Chave, J. (2020b) CCI Biomass project – In situ datasets: Processing and validation of NEON data (USA) (CCI Biomass internal report).

Labrière, N., & Chave, J. (2020c) In situ datasets: Processing and validation of TERN data (CCI Biomass internal report).

Lewis, S. L., Sonké, B., Sunderland, T., Begne, S. K., Lopez-Gonzalez, G., van der Heijden, G. M. F., . . . Zemagho, L. (2013). Above-ground biomass and structure of 260 African tropical forests. *Philosophical Transactions of the Royal Society B: Biological Sciences, 368*(1625), 20120295. https://doi.org/10.1098/rstb.2012.0295.

Mello, L. N. C., Sales, M. H. R., & Rosa, L. P. (2016). Analysis of results of biomass forest inventory in northeastern Amazon for development of REDD+ carbon project. *Anais da Academia Brasileira de Ciências, 88*, 55-64.

Menlove, J., & Healey, S. P. (2020). A Comprehensive Forest Biomass Dataset for the USA Allows Customized Validation of Remotely Sensed Biomass Estimates. *Remote Sensing*, *12*(24), 4141. https://doi.org/10.3390/rs12244141.

Mitchard, E. T. A., Saatchi, S. S., Lewis, S. L., Feldpausch, T. R., Gerard, F. F., Woodhouse, I. H., & Meir, P. (2011). Comment on 'A first map of tropical Africa's above-ground biomass derived from satellite imagery'. *Environmental Research Letters, 6*(4), 049001. https://doi.org/10.1088/1748-9326/6/4/049001.

Mitchard, E. T. A., Saatchi, S. S., Woodhouse, I. H., Nangendo, G., Ribeiro, N. S., Williams, M., . . . Meir, P. (2009). Using satellite radar backscatter to predict above-ground woody biomass: A consistent relationship across four different African landscapes. *Geophysical Research Letters, 36*(23). https://doi.org/10.1029/2009gl040692.

Morel, A. C., Saatchi, S. S., Malhi, Y., Berry, N. J., Banin, L., Burslem, D., . . . Ong, R. C. (2011). Estimating aboveground biomass in forest and oil palm plantation in Sabah, Malaysian Borneo using ALOS PALSAR data. *Forest Ecology and Management, 262*(9), 1786-1798. https://doi.org/10.1016/j.foreco.2011.07.008.

Paul, K. I., Roxburgh, S. H., Chave, J., England, J. R., Zerihun, A., Specht, A., . . . Sinclair, J. (2016). Testing the generality of above-ground biomass allometry across plant functional types at the continent scale. *Global Change Biology, 22*(6), 2106-2124. https://doi.org/10.1111/gcb.13201.

Pebesma, E.J. (2004). Multivariable geostatistics in S: the gstat package. Computers & Geosciences, 30: 683-691.

Planque, C, Punalekar, S, Lucas, R, Chognard, S, Owers, CJ, Clewley, D, Bunting, P, Sykes, H and Horton, C. (2020). Living Wales: Automatic and routine environmental monitoring using multi-source earth observation data. In K Schulz, U Michel and KG Nikolakopoulos (eds), Earth Resources and Environmental Remote Sensing/GIS Applications XI., 115340C, Proceedings of SPIE - The International Society for Optical Engineering, 11534, SPIE, Earth Resources and Environmental Remote Sensing/GIS Applications XI 2020. https://doi.org/10.1117/12.2573763

Ploton, P., MorTier, F., Barbier, N. et al. (2020). A map of African humid tropical forest aboveground biomass derived from management inventories. Sci Data 7, 221. https://doi.org/10.1038/s41597-020-0561-0.

Réjou-Méchain, M., Barbier, N., Couteron, P., Ploton, P., Vincent, G., Herold, M., . . . Pélissier, R. (2019). Upscaling Forest Biomass from Field to Satellite Measurements: Sources of Errors and Ways to Reduce Them. *Surveys in Geophysics*. https://doi.org/10.1007/s10712-019-09532-0.

Réjou-Méchain, M., Muller-Landau, H. C., Detto, M., Thomas, S. C., Le Toan, T., Saatchi, S. S., . . . Chave, J. (2014). Local spatial structure of forest biomass and its consequences for remote sensing of carbon stocks. *Biogeosciences, 11*(23), 6827-6840. https://doi.org/10.5194/bg-11-6827-2014.

Réjou-Méchain, M., Tanguy, A., Piponiot, C., Chave, J., & Hérault, B. (2017). biomass: an r package for estimating above-ground biomass and its uncertainty in tropical forests. *Methods in Ecology and Evolution, 8*(9), 1163-1167. https://doi.org/10.1111/2041-210X.12753.

Requena Suarez, D., Rozendaal, D. M. A., De Sy, V., Phillips, O. L., Alvarez-Dávila, E., Anderson-Teixeira, K., . . . Herold, M. (2019). Estimating aboveground net biomass change for tropical and subtropical forests: Refinement of IPCC default rates using forest plot data. *Global Change Biology, 25*(11), 3609-3624. doi:10.1111/gcb.14767

Rozendaal, D. M. A., M. Santoro, D. Schepaschenko, V. Avitabile and M. Herold (2017). DUE GlobBiomass D17 Validation Report, European Space Agency (ESA-ESRIN): 26.

Ryan, C. M., Berry, N. J., & Joshi, N. (2014). Quantifying the causes of deforestation and degradation and creating transparent REDD+ baselines: A method and case study from central Mozambique. *Applied Geography, 53*, 45-54. https://doi.org/10.1016/j.apgeog.2014.05.014.

Santoro, M., 2020. *CCI Biomass Product User Guide, Year 2, Version 2*. (CCI Biomass internal report).

Schepaschenko, D., Chave, J., Phillips, O. L., Lewis, S. L., Davies, S. J., Réjou-Méchain, M., . . . Zo-Bi, I. C. (2019). The Forest Observation System, building a global reference dataset for remote sensing of forest biomass. *Scientific Data, 6*(1), 198. https://doi.org/10.1038/s41597-019-0196-1.

Schepaschenko, D., Moltchanova, E., Fedorov, S., Karminov, V., Ontikov, P., Santoro, M., ... & Kraxner, F. (2021). Russian forest sequesters substantially more carbon than previously reported. *Scientific reports*, *11*(1), 1-7. https://doi.rog/10.1038/s41598-021-92152-9.

Ulander, L.M.H., Gustavsson, A., Flood, B., Murdin, D., Dubois-Fernandez, P., Dupuis, X., Sandberg, G., Soja, M.J., Eriksson, L.E.B., Fransson, J.E.S., Holmgren, J., Wallerman, J. (2011). BioSAR 2010 - Technical assistance for the development of airborne SAR and geophysical measurements during the BioSAR 2010 experiment.

Vaglio Laurin, G., Hawthorne, W., Chiti, T., Di Paola, A., Cazzolla Gatti, R., Marconi, S., . . . Valentini, R. (2016). Does degradation from selective logging and illegal activities differently impact forest resources? A case study in Ghana. [Does degradation from selective logging and illegal activities differently impact forest resources? A case study in Ghana]. *iForest - Biogeosciences and Forestry, 9*(3), 354-362. https://doi.org/10.3832/ifor1779-008.

Van Breugel, M., Bongers, F., & Martínez-Ramos, M. (2007). Species Dynamics During Early Secondary Forest Succession: Recruitment, Mortality and Species Turnover. *Biotropica, 39*(5), 610-619. https://doi.org/10.1111/j.1744-7429.2007.00316.x.

Vieilledent, G., Gardi, O., Grinand, C., Burren, C., Andriamanjato, M., Camara, C., . . . Rakotoarijaona, J.-R. (2016). Bioclimatic envelope models predict a decrease in tropical forest carbon stocks with climate change in Madagascar. *Journal of Ecology, 104*(3), 703-715. https://doi.org/10.1111/1365-2745.12548.

Willcock, S., Phillips, O. L., Platts, P. J., Balmford, A., Burgess, N. D., Lovett, J. C., . . . Lewis, S. L. (2014). Quantifying and understanding carbon storage and sequestration within the Eastern Arc Mountains of Tanzania, a tropical biodiversity hotspot. *Carbon Balance and Management, 9*(1), 2. https://doi.org/10.1186/1750-0680-9-2.

World Meteorological Organization (2011). Systematic observation requirements for satellite-based data products for climate: Supplemental details to the satellite-based component of the Implementation Plan for the Global Observing System for Climate in Support of the UNFCCC (2010 Update). https://library.wmo.int/doc_num.php?explnum_id=3710.

Appendix A - Details on the used forest plot data

ID	Tier	Average year	Average size (ha)	Count	Biome	URL	Paper/ source	Data access
AFR_L	3	2011	25.00	1	Tropical rainforest	https://dspace.stir.ac.uk/retrieve/74d3b352-fa46-418f-ba95-728bb33f4cfc/08417912.pdf	(Labrière et al., 2018)	open
EU_FOS	3	2014	16.25	1	Tropical rainforest	https://www.-ture.com/articles/s41597-019-0196-1?fbclid=IwAR08vLoOm4xEQo4EUdLtoKsnP6nsNIY5CYnfcoqGcS5Z0_UcyaNIr-jcdDg	(Schepaschenko et al., 2019)	open
SAM_L	3	2010	7.65	20	Tropical rainforest	https://dspace.stir.ac.uk/retrieve/74d3b352-fa46-418f-ba95-728bb33f4cfc/08417912.pdf	(Labrière et al., 2018)	open
AUS1	3	2009	25.00	1	Tropical dry forest	http://data.auscover.org.au/xwiki/bin/view/Product+pages/Biomass+Plot+Library	(Paul et al., 2016)	source-WUR agreement
SAM_RF	3	2008	5.3	10	Tropical rainforest	http://www.rainfor.org/en/project/about-rainfor	Lopez-Gonzales et al., 2011	Open
AFR_FOS	2	2013	1.00	44	Tropical rainforest	https://www.-ture.com/articles/s41597-019-0196-1?fbclid=IwAR08vLoOm4xEQo4EUdLtoKsnP6nsNIY5CYnfcoqGcS5Z0_UcyaNIr-jcdDg	(Schepaschenko et al., 2019)	open
AFR_L	2	2016	1.00	56	Tropical rainforest	https://dspace.stir.ac.uk/retrieve/74d3b352-fa46-418f-ba95-728bb33f4cfc/08417912.pdf	(Labrière et al., 2018)	open
AUS_FOS	2	2008	1.00	2	Tropical dry forest	https://www.-ture.com/articles/s41597-019-0196-1?fbclid=IwAR08vLoOm4xEQo4EUdLtoKsnP6nsNIY5CYnfcoqGcS5Z0_UcyaNIr-jcdDg	(Schepaschenko et al., 2019)	open
CAM_FOS	2	2012	1.01	18	Tropical rainforest	https://www.-ture.com/articles/s41597-019-0196-1?fbclid=IwAR08vLoOm4xEQo4EUdLtoKsnP6nsNIY5CYnfcoqGcS5Z0_UcyaNIr-jcdDg	(Schepaschenko et al., 2019)	open
EU_FOS	2	2010	2.23	2	Boreal coniferous forest	https://www.-ture.com/articles/s41597-019-0196-1?fbclid=IwAR08vLoOm4xEQo4EUdLtoKsnP6nsNIY5CYnfcoqGcS5Z0_UcyaNIr-jcdDg	(Schepaschenko et al., 2019)	open
SAM_FOS	2	2011	1.00	23	Tropical rainforest	https://www.-ture.com/articles/s41597-019-0196-1?fbclid=IwAR08vLoOm4xEQo4EUdLtoKsnP6nsNIY5CYnfcoqGcS5Z0_UcyaNIr-jcdDg	(Schepaschenko et al., 2019)	open
SAM_L	2	2013	1.04	28	Tropical rainforest	https://dspace.stir.ac.uk/retrieve/74d3b352-fa46-418f-ba95-728bb33f4cfc/08417912.pdf	(Labrière et al., 2018)	open

SAM_BAJ	2	2017	1	3	Tropical rainforest	https://ieeexplore.ieee.org/abstract/document/8518871	Pacheco-Pasccagaza et al., 2020	source-WUR agreement
SAM_RF	2	2008	1	374	Tropical rainforest	http://www.rainfor.org/en/project/about-rainfor	Lopez-Gonzales et al., 2011	Open
UK_FOS	2	2015	1.20	1	Tropical rainforest	https://www.-ture.com/articles/s41597-019-0196-1?fbclid=IwAR08vLoOm4xEQo4EUdLtoKsnP6nsNIY5CYnfcoqGcS5Z0_UcyaNIr-jcdDg	(Schepaschenko et al., 2019)	open
AFR10	2	2007	1.00	7	Tropical rainforest	https://iopscience.iop.org/article/10.1088/1748-9326/6/4/049001/meta	(Mitchard et al., 2011)	source-WUR agreement
AFR13	2	2008	1.00	2	Tropical rainforest	https://agupubs.onlinelibrary.wiley.com/doi/full/10.1029/2009GL040692	(Mitchard et al., 2009)	source-WUR agreement
AFR14	2	2009	1.63	4	Tropical rainforest	https://www.sciencedirect.com/science/article/abs/pii/S014362281400109X	(Ryan, Berry, & Joshi, 2014)	source-WUR agreement
AFR6	2	2009	1.00	12	Tropical rainforest	https://cbmjour-l.biomedcentral.com/articles/10.1186/1750-0680-9-2	(Willcock et al., 2014)	source-WUR agreement
AFR7	2	2012	1.00	19	Tropical rainforest	https://royalsocietypublishing.org/doi/full/10.1098/rstb.2012.0295	(Lewis et al., 2013)	source-WUR agreement
ASI3	2	2007	1.00	92	Tropical rainforest	https://www.sciencedirect.com/science/article/abs/pii/S0378112711004361	(Morel et al., 2011)	source-WUR agreement
AUS1	2	2012	1.01	63	Subtropical steppe	http://data.auscover.org.au/xwiki/bin/view/Product+pages/Biomass+Plot+Library	(Paul et al., 2016)	source-WUR agreement
SAM2	2	2012	1.00	40	Tropical rainforest	http://geoinfo.cnpm.embrapa.br/geonetwork/srv/ eng/main.home		source-WUR agreement
SAM_FOS	1	2011	0.25	142	Tropical rainforest	https://www.-ture.com/articles/s41597-019-0196-1?fbclid=IwAR08vLoOm4xEQo4EUdLtoKsnP6nsNIY5CYnfcoqGcS5Z0_UcyaNIr-jcdDg	(Schepaschenko et al., 2019)	open
AFR15	1	2013	0.25	136	Tropical rainforest	https://besjour-ls.onlinelibrary.wiley.com/doi/full/10.1111/1365-2745.12548%4010.1111/%28ISSN%291365-2745.FORESTRY	(Vieilledent et al., 2016)	source-WUR agreement
AFR1	1	2008	0.50	1152	Tropical rainforest	https://agritrop.cirad.fr/572060/1/document_572060.pdf	(Hirsh, Jourget, Feintrenie, Bayol,	source-WUR

							& Ebaá Atyi, 2013)	agreement
AFR10	1	2007	0.50	11	Tropical rainforest	https://iopscience.iop.org/article/10.1088/1748-9326/6/4/049001/meta	(Mitchard et al., 2011)	source-WUR agreement
AFR12	1	2008	0.16	108	Tropical rainforest	https://www.sciencedirect.com/science/article/abs/pii/S0034425711003609	(Avitabile, Baccini, Friedl, & Schmullius, 2012)	source-WUR agreement
AFR13	1	2008	0.50	23	Tropical rainforest	https://agupubs.onlinelibrary.wiley.com/doi/full/10.1029/2009GL040692	(Mitchard et al., 2009)	source-WUR agreement
AFR14	1	2009	0.51	70	Tropical dry forest	https://www.sciencedirect.com/science/article/abs/pii/S014362281400109X	(Ryan et al., 2014)	source-WUR agreement
AFR4	1	2012	0.13	110	Tropical mountain system	http://www.geo-informatie.nl/workshops/scw2/papers/deVries.pdf	(DeVries, Avitabile, Kooistra, & Herold, 2012)	source-WUR agreement
AFR5	1	2012	0.08	71	Tropical rainforest	https://pure.mpg.de/pubman/faces/ViewItemOverviewPage.jsp?itemId=item_2281402	(Vaglio Laurin et al., 2016)	source-WUR agreement
AFR6	1	2009	0.33	12	Tropical dry forest	https://cbmjour-l.biomedcentral.com/articles/10.1186/1750-0680-9-2	(Willcock et al., 2014)	source-WUR agreement
AFR8	1	2008	0.13	105	Tropical moist forest	https://www.sciencedirect.com/science/article/abs/pii/S0034425712001058	(Carreiras, Vasconcelos, & Lucas, 2012)	source-WUR agreement
AFR9	1	2016	0.13	9642	Tropical dry forest	https://www.mdpi.com/2072-4292/5/4/1524 https://fndsmoz.maps.arcgis.com/apps/MapSeries/index.html?appid=6602939f39ad4626a10f87bf6253af1e	(Carreiras et al., 2012)	open, source-WUR agreement
AFR_KEN	1	2011	0.09	362	Tropical and subtropical grasslands, savannas and shrublands			source-WUR agreement
ASI1	1	2008	0.05	2903	Tropical mountain system and rainforest	https://www.tandfonline.com/doi/full/10.1080/17583004.2016.1254009	(Avitabile et al., 2016)	source-WUR agreement

ASI10	1	2008	0.10	1268	Subtropical mountain system	https://www.sciencedirect.com/science/article/abs/pii/S0034425719303608	Zhang et al. 2019	source-WUR agreement
ASI2	1	2011	0.11	119	Tropical dry forest	http://www.leafasia.org/sites/default/files/public/resources/WWF-REDD-pres-July-2013-v3.pdf	WWF and OBf, 2013	source-WUR agreement
ASI4	1	2010	0.02	70	Tropical dry forest	http://citeseerx.ist.psu.edu/viewdoc/download?doi=10.1.1.972.708&rep=rep1&type=pdf	Wijaya et al., 2015	source-WUR agreement
ASI9	1	2012	0.13	74	Tropical rainforest	http://leutra.geogr.uni-je-.de/vgtbRBIS/metadata/start.php	Avitabile et al., 2014	source-WUR agreement
ASI_FOS	1	2014	0.25	2	Tropical rainforest	https://www.-ture.com/articles/s41597-019-0196-1?fbclid=IwAR08vLoOm4xEQo4EUdLtoKsnP6nsNIY5CYnfcoqGcS5Z0_UcyaNIr-jcdDg	(Schepaschenko et al., 2019)	open
AUS1	1	2011	0.12	5611	Tropical dry forest	http://data.auscover.org.au/xwiki/bin/view/Product+pages/Biomass+Plot+Library	Paul et al. 2016	source-WUR agreement
EU1	1	2011	0.01	16819	Temperate broadleaf and mixed forests and Boreal forests	https://www.slu.se/en/collaborative-centres-and-projects/swedish--tio-l-forest-inventory/	Sweden NFI	source-WUR agreement
EU2	1	2007	0.20	7177	Mediterranean forests	http://www.magrama.gob.es/es/desarrollo-rural/temas/politica-forestal/inventario-cartografia/inventario-forestal--cio-l/	Spain NFI	source-WUR agreement
EU3	1	2013	0.06	3021	Temperate oceanic forest	https://library.wur.nl/WebQuery/wurpubs/454875	Netherlands NFI	source-WUR agreement
EU4	1	2007	0.06	5967	Temperate broadleaf and mixed forests and Mediterranean forests	https://www.agriculturejour-ls.cz/publicFiles/01003.pdf	Cienciela et al. 2008	source-WUR agreement
EU_FOS	1	2015	0.28	514	Boreal forests	https://www.-ture.com/articles/s41597-019-0196-1?fbclid=IwAR08vLoOm4xEQo4EUdLtoKsnP6nsNIY5CYnfcoqGcS5Z0_UcyaNIr-jcdDg	(Schepaschenko et al., 2019)	open, source-WUR agreement
NAM1	1	2010	0.04	586	Boreal coniferous forest	https://www.p-s.org/content/112/18/5738.short	Liang et al., 2015	source-WUR agreement
NAM2	1	2004	0.04	75	Temperate mountain system	https://www.nature.com/articles/nature07276	Luyssaert et al., 2008	source-WUR agreement

NAM3	1	2010	0.03	588	Temperate continental forest			source-WUR agreement
NAM4	1	2010	0.04	2794	Temperate mountain system		Alaska NFI	source-WUR agreement
SAM2	1	2013	0.23	241	Tropical rainforest	https://www.paisagenslidar.cnptia.embrapa.br/webgis/	Embrapa, undated	source-WUR agreement
SAM3	1	2011	0.13	111	Tropical rainforest		CIFOR, undated	source-WUR agreement
SAM4	1	2014	0.15	7	Tropical rainforest		CIFOR, undated	source-WUR agreement
SAM5	1	2014	0.60	23	Tropical rainforest		CIFOR, undated	source-WUR agreement
SAM_BAJ	1	2017	0.25	363	Tropical rainforest	https://ieeexplore.ieee.org/abstract/document/8518871	Pacheco-Pasccagaza et al., 2020	source-WUR agreement
SAM_RF	1	2008	1	125	Tropical rainforest	http://www.rainfor.org/en/project/about-rainfor	Lopez-Gonzales et al., 2011	Open
SAM_TAPA	1	2009	0.5	138	Tropical rainforest	https://www.tandfonline.com/doi/full/10.1080/07038992.2014.913477?casa_token=EZxeZoegekkAAAAA%3AZHCN98XtpZRrsS9KoGTBhPy1_yzhAkkLZHfck3fomwSnvSaO7YDiuPV_hne6Mj1Wdn-7ME_sPChP	(Bispo et al., 2014)	source-WUR agreement
AFR_COF	0	2009	100	35029	Tropical moist forest,	https://www.nature.com/articles/s41597-020-0561-0	(Ploton et al., 2020)	open
LIDAR	0	2014	1	744397	Tropical rainforest		SLB, TERN, NEON	Open
LIDAR_SP	0	2017	1	54058	Temperate broadleaf and mixed forests and Mediterranean forests		(Gonzales et al., under preparation)	source-WUR agreement
EU_BEL	1	2013	0.1	688	Temperate broadleaf and mixed forests		Belgium TreeMort	source-WUR agreement

EU_BUL	1	2019	0.1	22	Temperate broadleaf and mixed forests		Dmitrov et al., under preparation	source-WUR agreement
EU_CZR	1	2014	0.1	25	Temperate conifer forests	https://www.sciencedirect.com/science/article/pii/S0925857416307182 https://www.mdpi.com/1999-4907/11/3/268	Brovkina et al., 2017; Novotny et al., 2020	source-WUR agreement
AFR_GHA	1	2010	0.1	94	Tropical rainforest	https://www.sciencedirect.com/science/article/pii/S0378112720310057	Brown et al., 2020	source-WUR agreement
EU_WLS	1	2016	0.5	134	Temperate broadleaf and mixed forests	https://www.forestresearch.gov.uk/tools-and-resources/national-forest-inventory/	Wales NFI	source-WUR agreement

Appendix B – Tables of assessments per biome

Table 29. Validation results for the boreal forests biome based on spatially aggregated data of all Tiers, LiDAR-based and CoFor AGB data.

		2010				2017					2018				
AGB_{ref} bin [Mg/ha]	# cells Count	AGB_{ref}	AGB_{map}	MD	$RMSD$	# cells count	AGB_{ref}	AGB_{map}	MD	$RMSD$	# cells count	AGB_{ref}	AGB_{map}	MD	$RMSD$
		------------------[Mg/ha] ----------------					-----------------[Mg/ha] --------------					-------------------[Mg/ha] -------------			
0-50	532	34	74	40	43	425	37	72	36	39	425	37	72	35	39
50-100	495	68	95	27	33	572	69	92	23	29	572	69	91	22	29
100-150	52	115	100	-15	25	70	114	99	-15	26	70	114	98	-16	28
total	1079	54	85	31	38	1067	59	85	26	33	1067	59	84	25	33

Table 30. Validation results for the mangroves biome based on spatially aggregated data of all Tiers, LiDAR-based and CoFor AGB data.

		2010				2017						2018				
AGB_{ref} bin [Mg/ha]	# cells count	AGB_{ref}	AGB_{map}	MD	$RMSD$	# cells count	AGB_{ref}	AGB_{map}	MD		$RMSD$	# cells count	AGB_{ref}	AGB_{map}	MD	$RMSD$
		------------------[Mg/ha] --------------						---------------------[Mg/ha] -----------					-------------------[Mg/ha] ------------			
0-50	62	31	50	20	41	18	38	59	21	56	18	18	38	59	21	57
50-100	32	65	65	1	36	32	71	67	-4	39	32	32	71	68	-3	42
100-150																
total	94	42	55	13	39	50	59	64	5	46	50	50	59	65	6	48

Table 31. Validation results for the Mediterranean forests, woodland and scrub biome based on spatially aggregated data of all Tiers, LiDAR-based and CoFor AGB data.

	2010					2017					2018				
AGB_{ref} bin	# cells	AGB_{ref}	AGB_{map}	*MD*	*RMSD*	# cells	AGB_{ref}	AGB_{map}	*MD*	*RMSD*	# cells	AGB_{ref}	AGB_{map}	*MD*	*RMSD*
[Mg/ha]	Count	[Mg/ha]				count	[Mg/ha]				count	[Mg/ha]			
0-50	2531	17	18	1	12	901	19	18	-1	15	901	19	16	-3	15
50-100	302	65	69	4	24	141	64	59	-6	24	141	64	55	-9	24
100-150	36	126	172	46	129	27	126	130	4	56	27	126	132	6	54
150-200	33	174	232	58	115	29	172	217	44	96	29	172	221	49	99
200-250	26	223	264	40	99	27	223	295	72	117	27	223	295	72	126
250-300	10	270	306	36	99	7	274	268	-6	85	7	274	263	-11	92
300-400	3	306	281	-25	55	3	305	303	-2	51	3	305	322	17	77
total	2941	28	31	3	26	1135	39	40	1	31	1135	39	38	-1	32

Table 32. Validation results for the temperate broadleaf and mixed forests biome based on spatially aggregated data of all Tiers, LiDAR-based and CoFor AGB data.

	2010					2017					2018				
AGB_{ref} bin [Mg/ha]	# cells Count	AGB_{ref}	AGB_{map}	*MD*	*RMSD*	# cells count	AGB_{ref}	AGB_{map}	*MD*	*RMSD*	# cells count	AGB_{ref}	AGB_{map}	*MD*	*RMSD*
		[Mg/ha]					[Mg/ha]					[Mg/ha]			
0-50	432	34	56	22	35	347	33	44	11	28	347	33	40	7	27
50-100	799	73	84	11	31	767	75	81	6	27	768	75	78	3	29
100-150	333	121	143	22	63	384	120	124	4	49	384	120	124	4	52
150-200	134	171	213	41	76	113	173	198	25	67	113	173	201	28	73
200-250	50	225	227	2	63	48	222	220	-1	68	48	222	224	2	76
250-300	21	276	230	-46	73	23	272	230	-42	66	24	273	238	-35	68
300-400	26	349	246	-103	117	24	348	242	-106	118	23	349	256	-93	109
>400	55	677	278	-399	483	52	696	266	-430	507	52	696	278	-418	497
total	1850	108	111	3	95	1758	111	104	-7	96	1759	111	103	-8	95

Table 33. Validation results for the temperate grasslands, savannas and shrublands biome based on spatially aggregated data of all Tiers, LiDAR-based and CoFor AGB data.

		2010					2017					2018			
AGB_{ref} bin [Mg/ha]	# cells Count	AGB_{ref}	AGB_{map}	*MD*	*RMSD*	# cells count	AGB_{ref}	AGB_{map}	*MD*	*RMSD*	# cells count	AGB_{ref}	AGB_{map}	*MD*	*RMSD*
		[Mg/ha]					[Mg/ha]					[Mg/ha]			
0-50	64	19	21	3	18	55	16	26	10	18	55	16	26	10	18
50-100	15	79	51	-28	35	11	76	75	-1	26	11	76	75	-1	26
100-150	10	118	93	-25	50	4	114	108	-7	16	4	114	108	-7	16
150-200	1	168	170	2	2	4	162	115	-47	49	4	162	115	-48	51
200-250	2	216	180	-36	49	74	38	43	5	22	74	38	42	4	22
total	92	45	39	-6	27	55	16	26	10	18	55	16	26	10	18

Table 34. Validation results for the tropical and subtropical dry broadleaf forest biome based on spatially aggregated data of all Tiers, LiDAR-based and CoFor AGB data.

		2010					2017					2018			
AGB_{ref} bin [Mg/ha]	# cells Count	AGB_{ref}	AGB_{map}	*MD*	*RMSD*	# cells count	AGB_{ref}	AGB_{map}	*MD*	*RMSD*	# cells count	AGB_{ref}	AGB_{map}	*MD*	*RMSD*
		[Mg/ha]					[Mg/ha]					[Mg/ha]			
0-50	25	30	106	76	92	15	37	99	63	83	15	37	99	62	82
50-100	40	75	95	20	50	25	75	138	62	95	25	75	134	59	93
100-150	18	125	110	-15	44	32	118	117	0	51	32	118	108	-10	50
150-200	15	171	118	-53	69	17	167	132	-35	65	17	167	131	-35	65
200-250	6	223	109	-113	115	6	222	144	-78	82	6	222	137	-85	90
250-300	3	263	162	-102	104	4	270	189	-81	88	4	270	174	-97	99
total	107	100	106	6	70	99	116	127	11	75	99	116	122	6	75

Table 35. Validation results for the tropical and subtropical grasslands, savannas and shrublands biome based on spatially aggregated data of all Tiers, LiDAR-based and CoFor AGB data.

	2010					2017					2018				
AGB_{ref} bin [Mg/ha]	# cells Count	AGB_{ref}	AGB_{map}	*MD*	*RMSD*	# cells count	AGB_{ref}	AGB_{map}	*MD*	*RMSD*	# cells count	AGB_{ref}	AGB_{map}	*MD*	*RMSD*
		[Mg/ha]					[Mg/ha]					[Mg/ha]			
0-50	166	26	30	4	36	59	25	30	6	52	54	24	30	6	53
50-100	114	70	46	-23	37	61	73	43	-30	37	64	72	42	-31	38
100-150	28	122	132	10	70	23	121	119	-2	56	22	121	113	-7	59
150-200	55	180	253	73	123	33	177	235	59	122	29	176	225	50	119
200-250	119	226	278	52	83	93	231	289	58	103	84	230	283	53	102
250-300	112	275	294	20	55	105	275	290	15	68	115	275	287	13	66
300-400	84	325	304	-21	63	122	331	314	-18	68	125	334	313	-21	69
>400	5	455	318	-136	151	3	476	315	-161	177	3	478	307	-172	184
total	683	165	177	12	66	499	214	224	10	77	496	217	222	5	75

Table 36. Validation results for the Tropical and subtropical moist broadleaf forest biome based on spatially aggregated data of all Tiers, LiDAR-based and CoFor AGB data.

		2010				2017					2018				
AGB_{ref} bin	# cells	AGB_{ref}	AGB_{map}	*MD*	*RMSD*	# cells	AGB_{ref}	AGB_{map}	*MD*	*RMSD*	# cells	AGB_{ref}	AGB_{map}	*MD*	*RMSD*
[Mg/ha]	Count	[Mg/ha]				count	[Mg/ha]				count	[Mg/ha]			
0-50	123	27	75	48	75	43	18	57	39	60	42	18	58	40	60
50-100	84	73	110	37	75	35	74	80	6	53	36	74	80	6	54
100-150	64	127	168	41	86	51	125	143	18	74	52	125	142	17	73
150-200	80	176	215	39	92	57	170	199	29	81	56	171	190	19	76
200-250	171	228	314	86	114	78	228	278	50	99	71	228	270	43	96
250-300	279	275	342	67	89	146	275	324	48	76	143	275	323	47	73
300-400	498	343	369	26	64	162	340	340	0	65	136	335	338	3	69
>400	80	432	357	-75	101	29	446	330	-116	143	13	457	310	-146	184
total	1379	256	296	40	84	601	242	262	20	79	549	230	252	22	78

Table 37. Validation results for the tundra biome based on spatially aggregated data of all Tiers, LiDAR-based and CoFor AGB data.

		2010				2017					2018				
AGB_{ref} bin	# cells	AGB_{ref}	AGB_{map}	*MD*	*RMSD*	# cells	AGB_{ref}	AGB_{map}	*MD*	*RMSD*	# cells	AGB_{ref}	AGB_{map}	*MD*	*RMSD*
[Mg/ha]	Count	[Mg/ha]				count	[Mg/ha]				count	[Mg/ha]			
0-50	72	32	56	23	28	72	30	52	23	28	72	30	53	23	29
50-100	34	71	72	1	19	45	67	70	3	20	45	67	71	4	21
100-150	6	115	60	-56	57	10	115	69	-47	52	10	115	70	-46	53
total	112	48	61	13	28	127	49	60	10	28	127	49	60	11	29